EUROPEAN ORGANISATION FOR NUCLEAR RESEARCH (CERN)

Phys. Rev. D 94, 032006 (2016)
DOI: 10.1103/PhysRevD.94.032006

CERN-EP-2016-051
October 21, 2016

Measurements of the charge asymmetry in top-quark pair production in the dilepton final state at $\sqrt{s} = 8$ TeV with the ATLAS detector

The ATLAS Collaboration

Abstract

Measurements of the top–antitop quark pair production charge asymmetry in the dilepton channel, characterized by two high-p_{T} leptons (electrons or muons), are presented using data corresponding to an integrated luminosity of 20.3 fb^{-1} from pp collisions at a center-of-mass energy $\sqrt{s} = 8$ TeV collected with the ATLAS detector at the Large Hadron Collider at CERN. Inclusive and differential measurements as a function of the invariant mass, transverse momentum, and longitudinal boost of the $t\bar{t}$ system are performed both in the full phase space and in a fiducial phase space closely matching the detector acceptance. Two observables are studied: $A_{\mathrm{C}}^{\ell\ell}$ based on the selected leptons and $A_{\mathrm{C}}^{t\bar{t}}$ based on the reconstructed $t\bar{t}$ final state. The inclusive asymmetries are measured in the full phase space to be $A_{\mathrm{C}}^{\ell\ell} = 0.008 \pm 0.006$ and $A_{\mathrm{C}}^{t\bar{t}} = 0.021 \pm 0.016$, which are in agreement with the Standard Model predictions of $A_{\mathrm{C}}^{\ell\ell} = 0.0064 \pm 0.0003$ and $A_{\mathrm{C}}^{t\bar{t}} = 0.0111 \pm 0.0004$.

Contents

1 Introduction

The top quark is the heaviest known elementary particle. Its large mass suggests that it may play a special role in theories of physics beyond the Standard Model (BSM) [1–5]. Such a role could be elucidated via precision tests of the Standard Model (SM) in large data samples of top–antitop quark pair ($t\bar{t}$) events collected at the Large Hadron Collider (LHC) in proton–proton (pp) collisions. One such test is the measurement of the charge asymmetry. The production of $t\bar{t}$ pairs at hadron colliders is symmetric under charge conjugation at leading order (LO) in quantum chromodynamics (QCD), i.e., the probability of a top quark flying in a given direction is the same as for an antitop quark [6]. At next-to-leading order (NLO) in QCD, an asymmetry arises from interference between different Feynman diagrams [3]. In particular, interference between the Born and one-loop diagram of the $q\bar{q} \to t\bar{t}$ processes and between $q\bar{q} \to t\bar{t}g$ diagrams with initial-state and final-state radiation (ISR and FSR) processes lead to a charge asymmetry. In the $t\bar{t}$ rest frame, this asymmetry causes the top quark to be preferentially emitted in the direction of the initial quark, and causes the antitop quark to be emitted in the direction of the initial antiquark. The size of the asymmetry can be enhanced by contributions beyond the SM, for example, $t\bar{t}$ production via the exchange of new heavy particles such as axigluons [3], heavy Z particles [4], or colored Kaluza–Klein excitations of the gluon [5].

Inclusive and differential measurements of the $t\bar{t}$ asymmetry were first performed at the Tevatron proton–antiproton collider, where forward-backward asymmetries were measured. Several measurements were reported by the CDF and D0 experiments [7–12] in dileptonic and semileptonic $t\bar{t}$ events. For these measurements, the direction of the initial quark can be assumed to be the direction of the proton, and the direction of the antiquark that of the antiproton, which yields straightforward access to the asymmetry. Initial tension between these measurements and theory predictions have been reduced with the latest SM calculations at next-to-next-to-leading order (NNLO) QCD [13].

Since the start of the LHC, measurements of $t\bar{t}$ charge asymmetries have been performed by the ATLAS and CMS experiments. Two features complicate the measurement of the asymmetry at the LHC: in proton–proton collisions the initial state is symmetric, so there is no $t\bar{t}$ forward-backward asymmetry, and the dominant production mechanism is gluon fusion, which is symmetric under charge conjugation to all orders in perturbative QCD. However, valence quarks carry on average a larger fraction of the proton momentum than sea antiquarks, hence top antiquarks produced through quark–antiquark annihilation are more central than top quarks [14]. By using differences between the absolute rapidity of the top and antitop quarks, ATLAS and CMS performed measurements of the charge asymmetry in dileptonic and semileptonic events at $\sqrt{s} = 7$ TeV and 8 TeV [15–22]. All asymmetry measurements at the LHC show good agreement with the SM prediction [23], which is approximately an order of magnitude smaller than the predicted asymmetry at the Tevatron.

In this article, new measurements of the charge asymmetry are presented using dileptonic $t\bar{t}$ events at $\sqrt{s} = 8$ TeV. The dileptonic channel is characterized by two charged leptons (denoted $\ell = e, \mu$), coming from either a direct vector boson decay or through an intermediate τ lepton decay. Two different observables are used, based either on the the selected leptons or the reconstructed $t\bar{t}$ final state. Inclusive and differential measurements as a function of the invariant mass of the $t\bar{t}$ system ($m_{t\bar{t}}$), the transverse momentum of the $t\bar{t}$ system ($p_{\mathrm{T},t\bar{t}}$), and the absolute value of the boost of the $t\bar{t}$ system along the beam axis ($\beta_{z,t\bar{t}}$) are performed. The inclusive and differential measurements are performed in the full phase space as well as in a fiducial volume based on the detector acceptance and selection requirements, using particle-level objects. The measurement in the fiducial region does not rely on extrapolating to regions of phase space that are not within the detector acceptance, while the full phase space measurement has the benefit of being comparable to theoretical calculations at the parton level, including BSM models.

In Sec. 2, a brief description of the ATLAS detector is given. Section 3 describes the data and Monte Carlo (MC) samples, and Sec. 4 the event selection and background estimation. The observables are described in Sec. 5. Section 6 outlines the measurement methods, including a description of the $t\bar{t}$ reconstruction, the definition of fiducial volume, and a description of the unfolding procedure. In Sec. 7, the sources of systematic uncertainties affecting the measurements are discussed, and results are provided in Sec. 8. Finally, conclusions are given in Sec. 9.

2 ATLAS detector

The ATLAS detector [24] at the LHC covers nearly the entire solid angle around the interaction point.[1] It consists of an inner tracking detector surrounded by a thin superconducting solenoid, electromagnetic and hadronic calorimeters, and a muon spectrometer incorporating superconducting toroid magnets.

[1] ATLAS uses a right-handed coordinate system with its origin at the nominal interaction point (IP) in the center of the detector and the z-axis along the beam pipe. The x-axis points from the IP to the center of the LHC ring, and the y-axis points upward. Cylindrical coordinates (r, ϕ) are used in the transverse plane, ϕ being the azimuthal angle around the beam pipe.

The inner-detector system is immersed in a 2 T axial magnetic field and provides charged-particle tracking in the pseudorapidity[2] range $|\eta| < 2.5$. A high-granularity silicon pixel detector covers the interaction region and provides typically three measurements per track. It is surrounded by a silicon microstrip tracker designed to provide four two-dimensional measurement points per track. These silicon detectors are complemented by a transition radiation tracker, which enables radially extended track reconstruction up to $|\eta| = 2.0$. The transition radiation tracker also provides electron identification information based on the fraction of hits (typically 30 in total) exceeding an energy-deposit threshold corresponding to transition radiation.

The calorimeter system covers the pseudorapidity range $|\eta| < 4.9$. Within the region $|\eta| < 3.2$, electromagnetic calorimetry is provided by barrel and endcap high-granularity lead/liquid-argon (LAr) electromagnetic calorimeters, with an additional thin LAr presampler covering $|\eta| < 1.8$ to correct for energy loss in the material upstream of the calorimeters. Hadronic calorimetry is provided by a steel/scintillator-tile calorimeter, segmented into three barrel structures within $|\eta| < 1.7$, and two copper/LAr hadronic endcap calorimeters. The solid angle coverage is completed with forward copper/LAr and tungsten/LAr calorimeters used for electromagnetic and hadronic measurements, respectively.

The muon spectrometer comprises separate trigger and high-precision tracking chambers measuring the deflection of muons in a magnetic field generated by superconducting air-core toroids. The precision chamber system covers the region $|\eta| < 2.7$ with drift tube chambers, complemented by cathode strip chambers. The muon trigger system covers the range of $|\eta| < 1.05$ with resistive plate chambers in the barrel, and the range of $1.05 < |\eta| < 2.4$ with thin gap chambers in the endcap regions.

A three-level trigger system is used to select interesting events. The Level-1 trigger is implemented in hardware and uses a subset of detector information to reduce the event rate to a design value of at most 75 kHz. This is followed by two software-based trigger levels, which together reduce the event rate to about 300 Hz.

3 Data and Monte Carlo samples

The data used for this analysis were collected during the 2012 LHC running period at a center-of-mass energy of 8 TeV. After applying data-quality selection criteria, the data sample used in the analysis corresponds to an integrated luminosity of 20.3 fb^{-1}.

For the modeling of the signal processes and most background contributions, several MC event generators are used. The main background contribution in this measurement comes from Drell–Yan production of $Z/\gamma^* \to \ell\ell$, which is estimated by a combination of simulated samples modified with corrections derived from data, as described in Sec. 4. The smaller contributions from diboson (WW, ZZ, and WZ) and single-top-quark (Wt channel) production are evaluated purely via MC simulations. Further background contributions can arise from events including a jet or a lepton from a semileptonic hadron decay misidentified as an isolated charged lepton as well as leptons from photon conversions, together referred to as "fake leptons". This contribution is estimated using simulated samples, modified with corrections derived from data. The samples mentioned above together with simulated samples of $t\bar{t} + W/Z$, t-channel of single-top-quark production, W+jets, and $W+\gamma$+jets are included in the estimation. The estimation procedure is described in Sec. 4.

[2] The pseudorapidity is defined in terms of the polar angle θ as $\eta = -\ln[\tan\theta/2]$, while the rapidity y is defined as $y = -(1/2)\ln[(E + p_z)/(E - p_z)]$.

The nominal $t\bar{t}$ signal sample is generated at NLO in QCD using POWHEG-hvq (version 1, r2330) [25–27] and the CT10 [28] parton distribution function (PDF) set, setting the h_{damp} parameter to the top-quark mass of 172.5GeV. The h_{damp} parameter is the resummation scale that is used in the damping function, which is designed to limit the resummation of higher-order effects at large transverse momentum without spoiling the NLO accuracy of the cross section. The parton shower, hadronization, and underlying event are simulated using PYTHIA6 (version 6.427) [29] with the CTEQ6L1 PDF [30] and the corresponding set of tunable parameters (Perugia 2011C tune [31]) intended to be used with this PDF. The $t\bar{t}$ cross section for pp collisions at a center-of-mass energy of 8 TeV is set to $\sigma_{t\bar{t}} = 253^{+13}_{-15}$ pb, calculated at NNLO in QCD including resummation of next-to-next-to-leading logarithmic (NNLL) soft gluon terms with top++2.0 [32–38]. The PDF and α_S uncertainties were calculated using the PDF4LHC prescription [39] with the MSTW2008 68% CL NNLO [40, 41], CT10 NNLO [42, 43], and NNPDF2.3 5f FFN [44] PDF sets, and added in quadrature to the scale uncertainty.

Single-top-quark production in the Wt channel is simulated using POWHEG-hvq with PYTHIA6 (version 6.426) and the CT10 (NLO) PDF set. The cross section of 22.3 ± 1.5 pb is estimated at approximate NNLO in QCD including resummation of NNLL terms [45]. The parton shower, hadronization, and underlying event are simulated by PYTHIA6 using the Perugia 2011C tune. The Drell–Yan process is modeled using ALPGEN (version 2.14) [46] interfaced with PYTHIA6 with the CTEQ6L1 [30] PDF set using the MLM matching scheme. Its heavy-flavor component is included in the matrix element calculations to model the $Z/\gamma^* + b\bar{b}$ and $Z/\gamma^* + c\bar{c}$ processes. Diboson processes (WW, ZZ, and WZ) are simulated using ALPGEN interfaced with HERWIG+JIMMY (version 4.31) [47, 48] with the CTEQ6L1 [30] PDF set for parton fragmentation [49]. The only exceptions are the same-charge $W^{+(-)}W^{+(-)}$ samples, which are simulated using MADGRAPH (version 5.1.4.8) [50] interfaced with PYTHIA8 (version 8.165) [51]. The samples are normalized to the reference NLO QCD prediction, obtained using the MCFM generator [52]. The associated production of a $t\bar{t}$ pair with a vector boson ($t\bar{t}Z$ and $t\bar{t}W$) is simulated with MADGRAPH interfaced with PYTHIA8 and normalized to NLO cross-section calculations [53, 54]. The W+jets events are simulated using ALPGEN interfaced with PYTHIA6 and the $W+\gamma$+jets process is simulated using ALPGEN interfaced with JIMMY.

To model the LHC environment properly, additional inelastic pp collisions are generated with PYTHIA8 and overlaid on the hard process. All the simulated samples are then processed through a simulation of the ATLAS detector [55]. For most of the samples, a full simulation based on GEANT4 [56] is used. Some of the samples used to evaluate the generator modeling uncertainties are obtained using a faster detector simulation where only the calorimeter simulation is modified and relies on parametrized showers [57]. The simulated events are passed through the same reconstruction and analysis chain as data.

4 Event selection and background estimation

In order to enrich the data sample in dileptonic $t\bar{t}$ events, requirements are imposed on reconstructed charged leptons (electrons and muons), jets, and the missing transverse momentum. Three different final states are considered in the analysis: events with two electrons in the final state (ee), with one electron and one muon ($e\mu$), and with two muons ($\mu\mu$).

Electron candidates are reconstructed from an electromagnetic calorimeter energy deposit matched to a track in the inner detector and must pass the likelihood-based "medium" identification requirements [58]. They are required to have transverse momentum $p_T > 25$ GeV and must also lie in the region $|\eta_{\text{cl}}| < 2.47$, where η_{cl} is the pseudorapidity of the calorimeter energy cluster associated with the electron, excluding

the transition region between the calorimeter barrel and endcaps $1.37 < |\eta_{\mathrm{cl}}| < 1.52$. Moreover, electrons are required to be isolated from surrounding activity in the inner detector. The scalar sum of the track p_{T} within a cone of $\Delta R = \sqrt{(\Delta\eta)^2 + (\Delta\phi)^2} = 0.3$ (excluding the track of the electron itself) divided by the electron p_{T} should be less than 0.12.

Muon candidates are reconstructed using combined information from the muon spectrometer and the inner detector [59]. They are required to have $p_{\mathrm{T}} > 25$GeV and $|\eta| < 2.5$. In addition, muons are required to satisfy track-based p_{T}-dependent isolation criteria. The scalar sum of the track p_{T} within a cone of size $\Delta R = 10\ \mathrm{GeV}/p_{\mathrm{T}}^{\mu}$ around the muon (excluding the muon track itself) must be less than 5% of the muon p_{T} (p_{T}^{μ}). Both the electrons and muons have to be consistent with the primary vertex,[3] by requiring the absolute value of the longitudinal impact parameter to be less than 2 mm.

Jets are reconstructed from clustered energy deposits in the electromagnetic and hadronic calorimeters, using the anti-k_t [60] algorithm with a radius parameter $R = 0.4$. The measured energy of the jets is corrected to the hadronic scale using p_{T}- and η-dependent scale factors derived from simulation and validated in data [61]. After the energy correction, the jets are required to have $p_{\mathrm{T}} > 25$GeV, to be in the pseudorapidity range $|\eta| < 2.5$, and to have a jet vertex fraction $|\mathrm{JVF}| > 0.5$ [62] if $p_{\mathrm{T}} < 50$GeV. The jet vertex fraction is defined as the summed scalar p_{T} of the tracks associated with both the jet and the primary vertex divided by the summed scalar p_{T} of all tracks in the jet. The jet that is the closest to a selected electron is removed from the event if their separation is $\Delta R < 0.2$. After this jet overlap removal, electrons and muons that are within a cone of $\Delta R = 0.4$ around the closest jet are removed. Jets containing b-hadrons are identified (b-tagged) using a multivariate algorithm (MV1) [63]. This is a neural-network-based algorithm that makes use of track impact parameters and reconstructed secondary vertices. Jets are identified as b-tagged jets by requiring the MV1 output discriminant to be above a certain threshold value. This value is chosen such that the overall tagging efficiency for b-jets with $p_{\mathrm{T}} > 20$GeV and $|\eta| < 2.5$ originating from top-quark decays in dileptonic MC $t\bar{t}$ events is 70%. The rejection factor for jets originating from gluons and light quarks is about 130, while for c-quarks it is about 5.

The magnitude of the missing transverse momentum ($E_{\mathrm{T}}^{\mathrm{miss}}$) is calculated from the negative vector sum of all calorimeter energy deposits and the momenta of muons [64]. The calculation is refined by the application of the object-level corrections for the contributions arising from identified electrons and muons.

Events recorded with single-lepton triggers (e or μ) under stable beam conditions with all detector subsystems operational are considered. The transverse momentum thresholds are 24 GeV for isolated single-lepton triggers and 60 (36) GeV for nonisolated single-electron (single-muon) triggers. The nonisolated triggers are used to select events that fail the isolation requirement at trigger level but pass it in the offline analysis. In all three final states, exactly two isolated leptons with opposite charge and an invariant mass $m_{\ell\ell} > 15$ GeV are required, together with at least two jets. In the same-flavor channels (ee and $\mu\mu$), the invariant mass of the two charged leptons is required to be outside of the Z boson mass window such that $|m_{\ell\ell} - m_Z| > 10$ GeV. Furthermore, it is required that $E_{\mathrm{T}}^{\mathrm{miss}} > 30$ GeV and at least one of the jets must be b-tagged. These requirements suppress the dominant background contribution from Drell–Yan production of $Z/\gamma^* \to \ell\ell$ and also suppress diboson backgrounds. In the $e\mu$ channel, the background contamination is much smaller and the background suppression is achieved by requiring the scalar sum of the p_{T} of the two leading jets and leptons (H_{T}) to be larger than 130 GeV. The event selection requirements are summarized in Table 1.

[3] The primary vertex is defined as the reconstructed vertex with at least five associated tracks (of $p_T > 0.4$ GeV) and the highest sum of the squared transverse momenta of the associated tracks.

Table 1: The summary of the event selection requirements applied in different channels.

Requirements	$ee/\mu\mu$	$e\mu$
Leptons	2	2
Jets	≥ 2	≥ 2
$m_{\ell\ell}$	> 15 GeV	> 15 GeV
$\lvert m_{\ell\ell} - m_Z \rvert$	> 10 GeV	–
$E_{\mathrm{T}}^{\mathrm{miss}}$	> 30 GeV	–
b-tagged jets	≥ 1	–
H_{T}	–	> 130 GeV

The modeling of Drell–Yan events in the same-flavor channels with $E_{\mathrm{T}}^{\mathrm{miss}} > 30$ GeV may not be accurate in simulation due to the mismodeling of the $E_{\mathrm{T}}^{\mathrm{miss}}$ distribution. Moreover, after applying the b-tagging requirement, a large contribution to the background comes from the associated production of Z bosons with heavy-flavor jets, which is not well predicted by MC simulation. The first source of mismodeling depends on the reconstructed objects and is therefore different in each channel. The second source is a limitation of the MC simulation and is expected to be the same in both channels. Thus, the normalization of the inclusive and heavy-flavor component of the Drell-Yan background in the same-flavor channels is computed simultaneously using data in two control regions with three scale factors. Two scale factors are applied to all Drell–Yan events to take into account the mismodeling from the $E_{\mathrm{T}}^{\mathrm{miss}}$ requirement (one in the ee and one in the $\mu\mu$ channel) while another is applied only to Z+heavy-flavor events. The control regions are defined using the standard selection described previously but inverting the $m_{\ell\ell}$ cut to be within the Z mass window. The first control region is defined without the b-tagging requirement while the second is defined with at least one b-tagged jet. The simulated $m_{\ell\ell}$ distribution in these control regions is simultaneously fit to the data and the scale factors are extracted. The scale factors derived in these two regions are 0.927 ± 0.005 and 0.890 ± 0.004 for the ee and $\mu\mu$ channels, respectively, and 1.70 ± 0.03 for the heavy-flavor component. The $Z \to \tau\tau$ process in the $e\mu$ channel is estimated using MC simulation only: no data-driven correction is applied since neither the $E_{\mathrm{T}}^{\mathrm{miss}}$ requirement nor b-tagging requirement are applied to this channel.

The background arising from misidentified and nonprompt (NP) leptons is determined using both MC simulation and data. The dominant sources of these fake leptons are semileptonic b-hadron decays, long-lived weakly decaying states (such as $\pi^{\pm}$ or $K^{\pm}$ mesons), π^0 showers, photons reconstructed as electrons, and electrons from photon conversions. W+jets, W+γ+jets, $t\bar{t}$, $t\bar{t}Z$, $t\bar{t}W$, Drell–Yan, single-top-quark, and diboson production are taken into account for the estimation of this background. Multijet events do not contribute significantly to this background, since the probability of having two jets misidentified as isolated leptons is very small. The shapes of the kinematic distributions are taken from simulated events where at least one of two selected leptons is required not to be matched with the MC generator-level leptons. Scale factors are derived from data in order to adjust the normalization. A control region, enriched in fake leptons, is defined by applying the same cuts as for the final selection but requiring the two leptons to have the same charge. The shapes of the distributions for various kinematic variables of leptons, jets, and $E_{\mathrm{T}}^{\mathrm{miss}}$ are checked and found to be well modeled in the MC simulation. The scale factors are derived in this region by comparing data and simulation and are then applied to the simulated events in the signal region. The scale factor is 1.2 ± 0.3 in the ee channel, 1.1 ± 0.2 in the $e\mu$ channel, and 3.7 ± 0.8 in the $\mu\mu$ channel, where the uncertainties are statistical. The sources of misidentified muons, such as heavy-flavor decays, are quite different from those of misidentified electrons. The large difference

between the scale factor for the $\mu\mu$ and the $e\mu$ channel is mainly due to the b-tagging requirement, that is applied only in the $\mu\mu$ channel. However, the shapes of the distributions of the relevant kinematic variables in the $\mu\mu$ channel are cross-checked in control regions and found to be consistent with the distributions from a purely data-driven method. The systematic uncertainties of both Drell–Yan background and the background due to events from misidentified and nonprompt leptons are discussed in detail in Sec. 7.2.

The numbers of events for both expectation and data after applying the selection criteria are shown in Table 2 for the three final states. The uncertainties shown correspond to the total uncertainty (including the statistical uncertainties from the limited size of the MC simulated samples, as well as the systematic uncertainties). The $e\mu$ channel contributes with the largest number of events, followed by $\mu\mu$ and ee. Figure 1 shows good agreement within the systematic uncertainties between data and the predictions as a function of jet multiplicity, lepton p_T and η, for all channels combined.

Table 2: Observed numbers of data events compared to the expected signal and background contributions in the three decay channels. The uncertainty corresponds to the total uncertainty in the given process. Data-driven (DD) scale factors are applied to the Z+jets and the NP & fake leptons contributions. The $Z \to \tau\tau$ process in the $e\mu$ channel is estimated using MC simulation only.

Channel	ee	$\mu\mu$	$e\mu$
$t\bar{t}$	10200 ± 800	12100 ± 800	36000 ± 2400
Single-top	510 ± 50	590 ± 50	1980 ± 170
Diboson	31 ± 5	40 ± 6	1320 ± 100
$Z \to ee$ (DD)	1200 ± 260	–	–
$Z \to \mu\mu$ (DD)	–	1520 ± 300	–
$Z \to \tau\tau$ (DD/MC)	31 ± 15	58 ± 25	1120 ± 430
NP & fake leptons (DD)	$62\ ^{+119}_{-29}$	$45\ ^{+36}_{-24}$	$480\ ^{+240}_{-220}$
Total Expected	12000 ± 900	14400 ± 800	40900 ± 2500
Data	12785	14453	42363

5 Observables

In dileptonic events, the charge asymmetry can be measured in two complementary ways: using the pseudorapidity of the charged leptons or using the rapidity of the top quarks. The asymmetry based on the charged leptons uses the difference of the absolute pseudorapidity values of the positively and negatively charged leptons, $|\eta_{\ell^+}|$ and $|\eta_{\ell^-}|$

$$\Delta|\eta| = |\eta_{\ell^+}| - |\eta_{\ell^-}|. \tag{1}$$

The leptonic asymmetry is defined as

$$A_{\mathrm{C}}^{\ell\ell} = \frac{N(\Delta|\eta| > 0) - N(\Delta|\eta| < 0)}{N(\Delta|\eta| > 0) + N(\Delta|\eta| < 0)}, \tag{2}$$

where $N(\Delta|\eta| > 0)$ and $N(\Delta|\eta| < 0)$ represent the number of events with positive and negative $\Delta|\eta|$, respectively. The SM prediction at NLO in QCD, including electroweak corrections, is $A_{\mathrm{C}}^{\ell\ell} = 0.0064 \pm 0.0003$ [23], where the uncertainty includes variations in scale and choice of PDF. The leptonic asymmetry, that is slightly diluted with respect to the underlying top-quark asymmetry, has the advantage that no

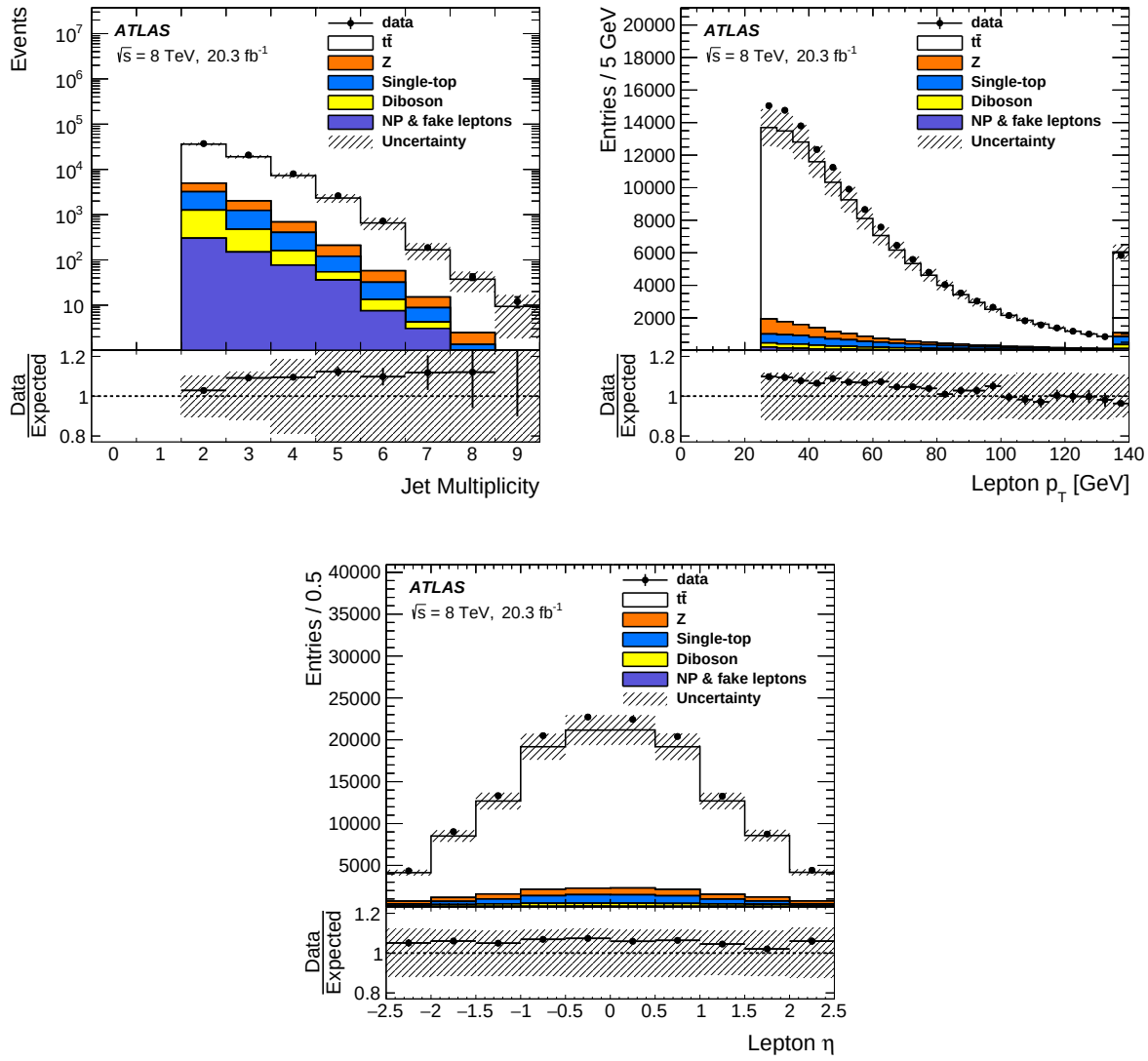

Figure 1: Distributions of the jet multiplicity, lepton p_T, and lepton η for data (points) and predictions (histograms) for all channels combined after event selection. The data/expected ratio is also shown. The shaded area corresponds to the detector systematic uncertainty, the signal modeling systematic uncertainty, and the normalization uncertainty in signal and background. In the lepton p_{T} distribution, the last bin includes the overflow.

reconstruction of the top–antitop quark system is required. Furthermore, it is also sensitive to top-quark polarization effects, which occur in some models predicting enhanced charge asymmetries.

For the $t\bar{t}$ charge asymmetry, the $t\bar{t}$ system has to be reconstructed and the absolute values of the top and antitop quark rapidities ($|y_t|$ and $|y_{\bar{t}}|$, respectively) need to be computed. Using

$$\Delta|y| = |y_t| - |y_{\bar{t}}|, \tag{3}$$

the $t\bar{t}$ charge asymmetry is defined as

$$A_{\mathrm{C}}^{t\bar{t}} = \frac{N(\Delta|y| > 0) - N(\Delta|y| < 0)}{N(\Delta|y| > 0) + N(\Delta|y| < 0)}, \tag{4}$$

where $N(\Delta|y| > 0)$ and $N(\Delta|y| < 0)$ represent the number of events with positive and negative $\Delta|y|$, respectively. The top (antitop) quarks are identified as those giving rise to positive (negative) leptons. The SM prediction at NLO QCD, including electroweak corrections, is $A_{\mathrm{C}}^{t\bar{t}} = 0.0111 \pm 0.0004$ [23].

The measurements of $A_{\mathrm{C}}^{\ell\ell}$ and $A_{\mathrm{C}}^{t\bar{t}}$ are performed inclusively and differentially as a function of $m_{t\bar{t}}$, $p_{\mathrm{T},\mathrm{t}\bar{\mathrm{t}}}$, and $\beta_{z,t\bar{t}}$. The fractions of quark–antiquark annihilation and gluon fusion processes change as a function of $m_{t\bar{t}}$, and thus an increasing asymmetry for increasing $m_{t\bar{t}}$ is expected. Since $p_{\mathrm{T},\mathrm{t}\bar{\mathrm{t}}}$ depends on the initial-state radiation, the asymmetry value is expected to change as a function of $p_{\mathrm{T},\mathrm{t}\bar{\mathrm{t}}}$. In particular, the contribution to the asymmetry from interference of diagrams with initial- and final-state radiation is negative, resulting in decreasing asymmetries with increasing $p_{\mathrm{T},\mathrm{t}\bar{\mathrm{t}}}$. While the initial antiquark is always a sea quark, the initial quark can be a valence quark. On average, valence quarks have higher momenta than sea quarks, which can result in a boost of the $t\bar{t}$ system in the direction of the incoming quark. This results in an increased charge asymmetry for increasing $\beta_{z,t\bar{t}}$. The asymmetry is also expected to be different inclusively and differentially in different BSM models.

6 Asymmetry measurements

The following measurements are performed:

- inclusive measurements of the $t\bar{t}$ and leptonic asymmetries, corrected for reconstruction and acceptance effects to parton level in the full phase space;
- inclusive measurements of the $t\bar{t}$ and leptonic asymmetries, corrected for reconstruction effects to particle level in the fiducial region;
- differential measurements of the $t\bar{t}$ and leptonic asymmetries as a function of $m_{t\bar{t}}$, $p_{\mathrm{T},\mathrm{t}\bar{\mathrm{t}}}$, and $\beta_{z,t\bar{t}}$ in the fiducial region and the full phase space.

Particle-level results consider stable particles with a mean lifetime larger than 0.3×10^{-10} s. For the parton-level measurements, MC generator-level objects are used. The parton-level top quarks and leptons are selected after radiation.

The leptonic asymmetry can be extracted directly using the pseudorapidities of the measured charged leptons. For the $t\bar{t}$ charge asymmetry, the reconstruction of the top and antitop quark four-momenta is necessary. A kinematic method is used for the reconstruction, as described in Sec. 6.1. Section 6.2 details the definition of the fiducial volume and the particle-level objects used for the fiducial measurement. In order to correct the measured asymmetry distributions for detector and acceptance effects, an unfolding

method, described in Sec. 6.3, is used for all asymmetry measurements. Section 6.4 describes how the various asymmetries are extracted.

6.1 Top and antitop quark reconstruction

For the reconstruction of the top and antitop quark four-momenta, a kinematic reconstruction is used. The reconstruction is performed by solving the system of equations that relate the particle momenta at each of the decay vertices in the $t\bar{t} \to W^+bW^-\bar{b} \to \ell^+\nu_\ell b\ell^-\bar{\nu}_\ell\bar{b}$ process. Two neutrinos are produced and escape undetected. Thus, an underconstrained system is obtained. This system is solved using the kinematic (KIN) method [65, 66], assuming values of 172.5 GeV and 80.4 GeV for the top quark and W boson masses, respectively, which allows the system of equations to be solved numerically by the Newton–Raphson method.

If there are more than two reconstructed jets in a given event, the two jets with the highest b-tagging weights (as determined by the MV1 b-tagging algorithm) are used. This improves the probability of choosing the correct jets, compared to just choosing the two jets with the highest p_T, from about 54% to about 69% in the inclusive selected sample. The experimental uncertainties of the measured objects (described in Sec. 7) are taken into account by sampling the phase space of the measured jets and $E_{\mathrm{T}}^{\mathrm{miss}}$ according to their resolution in simulation. The number of sampled points is called N_{smear}, whose optimization is based on the time and efficiency of the top-pair reconstruction. The resolution functions, obtained from the $t\bar{t}$ simulated sample, with respect to the jet p_{T} (for jets) and the total transverse momentum in the event (for $E_{\mathrm{T}}^{\mathrm{miss}}$) are used for the sampling.

For each sampling point, up to four solutions can be obtained. The KIN method chooses the solution that leads to the lowest reconstructed mass of the $t\bar{t}$ system. The reason for this is that the $t\bar{t}$ cross section is a decreasing function of the partonic center-of-mass energy $\sqrt{\hat{s}} \simeq m_{t\bar{t}}$, so events with smaller $m_{t\bar{t}}$ are more likely. There is also a twofold ambiguity in the lepton and b-jet assignment. The correct assignment to the top and antitop quarks is chosen to be the one that has more reconstructed trials $N_{\mathrm{smear}}^{\mathrm{reco}}$, i.e., the one that maximizes $N_{\mathrm{smear}}^{\mathrm{reco}}/N_{\mathrm{smear}}$. The chosen solution is either the solution found using the nominal jet energies and measured $E_{\mathrm{T}}^{\mathrm{miss}}$, if available, or the first solution found during the sampling. The kinematic reconstruction fails for a given event if no solution is found in any of the N_{smear} sampled points. This is possible if, for example, the solution does not converge within a given number of iterations. The performance of the method is quantified by evaluating the efficiency of reconstructing $t\bar{t}$ events that pass dilepton event selection, and the probability of reconstructing the correct sign of $\Delta|y|$. These probabilities are found to be 90% and 76%, respectively. The reconstruction efficiency is consistent between data and the prediction.

Figure 2 shows the distributions for data and prediction of the p_T, mass, and longitudinal boost of the $t\bar{t}$ system after applying the reconstruction method. Good agreement between data and prediction is found.

6.2 Particle-level objects and fiducial region

A fiducial region is defined in order to closely match the phase space region accessed with the ATLAS detector and the requirements made on the reconstructed objects. A fiducial measurement usually allows for MC generator dependencies to be reduced, since it avoids large extrapolation to the full phase space. In the fiducial region, only objects defined at particle level are used.

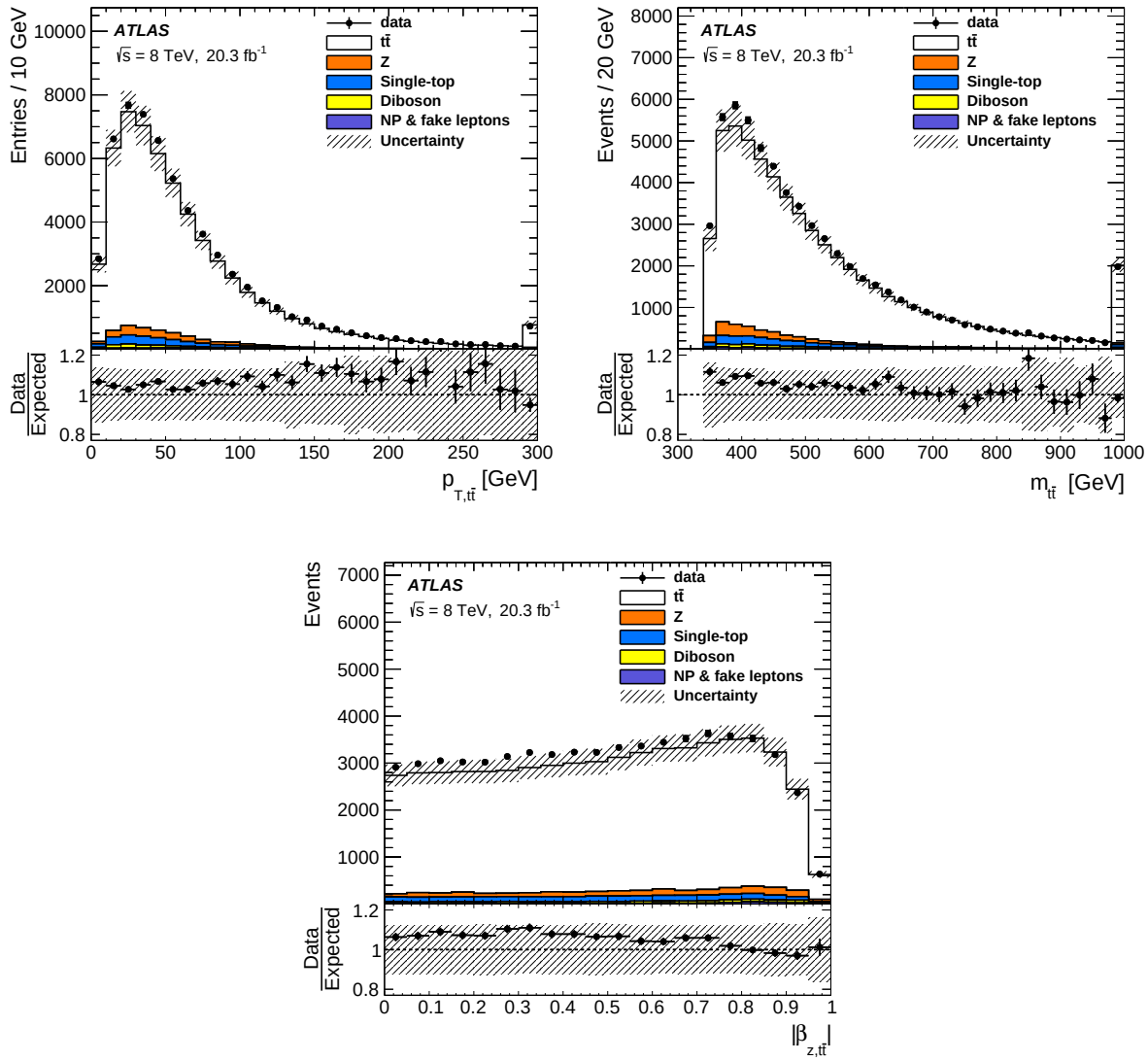

Figure 2: Distributions of $p_{\mathrm{T},t\bar{t}}$, $m_{t\bar{t}}$, and $|\beta_{z,t\bar{t}}|$ for data (points) and predictions (histograms) after kinematic reconstruction. The data/expected ratio is also shown. The shaded area corresponds to the detector systematic uncertainty, the signal modeling systematic uncertainty, and the normalization uncertainty in signal and background. In the $p_{\mathrm{T},t\bar{t}}$ and $m_{t\bar{t}}$ distributions, the last bin includes the overflow.

The considered charged leptons (electrons and muons) are required not to originate from hadrons. Photons within $\Delta R = 0.1$ around the charged lepton are included in the four-momentum calculation. The $E_{\mathrm{T}}^{\mathrm{miss}}$ is calculated as the summed four-momenta of neutrinos from the W/Z boson decays, including those from τ decays. Jets are reconstructed using the anti-k_t algorithm with a radius parameter $R = 0.4$. The electrons, muons, neutrinos, and photons that are used in the definition of the selected leptons are excluded from the clustering. Finally, identification of jets originating from b-quarks is achieved using ghost matching [67]. The MC generator-level b-hadrons are clustered into the particle-level jets, with their momenta scaled to a very small value. If a clustered jet is found to contain a b-hadron, the particle-level jet is labelled as a b-jet.

The fiducial volume is defined by requiring at least two particle-level jets and at least two leptons in the event, both objects with $p_T > 25$ GeV and $|\eta| < 2.5$. Events where leptons and jets overlap, within ΔR of 0.4, are rejected. The particle-level jets are not required to be b-jets since this requirement is not shared between the three channels in the selection.

Using these objects, the reconstruction of top quarks (known as pseudotops [68]) can be performed. The assignment of the proper jet-lepton-neutrino permutation is chosen by first minimizing the difference between the mass computed from each lepton-neutrino combination and the W boson mass value used in the MC simulation. Then, the difference between the mass of each combination of the chosen lepton-neutrino pairs with a jet and the top quark mass value, used in the MC simulation, is minimized. The b-jets are prioritized over the light jets for the proper jet-lepton-neutrino assignment. The correlation coefficient between $\Delta|y|$ at the parton and particle levels is found to be 79%, while for $\Delta|\eta|$ it is 99%.

The measurements of the asymmetry in the fiducial volume require the treatment of an additional background contribution, in which signal events from outside of the fiducial region migrate into the detector acceptance due to resolution effects. This nonfiducial background constitutes about 8% of the expected $t\bar{t}$ events after selection, as estimated by using MC simulation, and it was found to be independent of the charge asymmetry value of the simulated sample. A bin-by-bin scale factor derived from simulation is applied to background-subtracted data to estimate the contribution of these events.

6.3 Unfolding

The measurements are corrected for detector resolution and acceptance effects. These corrections are performed using the fully Bayesian unfolding (FBU) technique [69]. The FBU procedure applies Bayes' theorem to the problem of unfolding. This application can be stated in the following terms: given an observed spectrum $\boldsymbol{D}$ with N_r reconstructed bins and a migration matrix $\mathcal{M}$ with $N_r \times N_t$ bins giving the detector response to a true spectrum with N_t bins, the posterior probability of the true spectrum $\boldsymbol{T}$ with N_t bins follows the probability density

$$p(\boldsymbol{T}|\boldsymbol{D}) \propto \mathcal{L}(\boldsymbol{D}|\boldsymbol{T}) \cdot \pi(\boldsymbol{T}), \tag{5}$$

where $\mathcal{L}(\boldsymbol{D}|\boldsymbol{T})$ is the likelihood of $\boldsymbol{D}$ assuming $\boldsymbol{T}$ and $\mathcal{M}$, and π is the prior probability density for the true spectrum $\boldsymbol{T}$. The selection and reconstruction efficiency, which is the probability that an event produced in MC generator-level bin t is reconstructed in one of the N_r bins included in $\mathcal{M}$, is taken into account in the likelihood. An uninformative prior probability density is chosen, such that equal probabilities are assigned to all $\boldsymbol{T}$ spectra within a wide range. The background in each bin is taken into account when computing $\mathcal{L}(\boldsymbol{D}|\boldsymbol{T})$. The unfolded spectrum and its associated uncertainty are extracted from the posterior probability density distribution.

The migration matrix is obtained from the nominal $t\bar{t}$ simulated sample using the top quarks before their decay (parton level) or pseudotops (particle level). The combination of the three decay channels is performed by using a rectangular migration matrix, which maps the reconstructed distribution of the three channels to the same corrected distribution.

To validate the method, a linearity test is performed for the inclusive and differential measurements of the charge asymmetry. A given asymmetry value is introduced by reweighting the samples according to a nonlinear function of $\Delta|y|$ and $\Delta|\eta|$ based on a BSM axigluon model [70]. The asymmetry values are in the range of -6% to 6% in steps of 2%. Good agreement between the unfolded values and the injected values is found, and the calibration curves derived from this test are linear.

For the treatment of systematic uncertainties in the Bayesian inference approach, the likelihood $\mathcal{L}(\boldsymbol{D}|\boldsymbol{T})$ is extended with nuisance parameter terms. This marginal likelihood is defined as

$$\mathcal{L}(\boldsymbol{D}|\boldsymbol{T}) = \int \mathcal{L}(\boldsymbol{D}|\boldsymbol{T},\boldsymbol{\theta}) \cdot \pi(\boldsymbol{\theta}) d\boldsymbol{\theta}\,, \tag{6}$$

where $\boldsymbol{\theta}$ are the nuisance parameters, and $\pi(\boldsymbol{\theta})$ their prior probability densities, which are assumed to be normal distributions $\mathcal{N}$ with a mean value of zero and a variance of one. A nuisance parameter is associated with each of the uncertainty sources. As is described in Sec. 7, four categories of uncertainties are considered in this analysis, but only two are included in the marginalization: the normalizations of the background processes ($\boldsymbol{\theta}_b$), and the uncertainties associated with the object identification, reconstruction and calibration ($\boldsymbol{\theta}_s$). While the first ones only affect the background predictions, the latter, referred to as object systematic uncertainties, affect both the reconstructed distribution for the $t\bar{t}$ signal ($\boldsymbol{R}(\boldsymbol{T};\boldsymbol{\theta}_s)$) and the total background prediction ($\boldsymbol{B}(\boldsymbol{\theta}_s,\boldsymbol{\theta}_b)$). The marginal likelihood then becomes

$$\mathcal{L}(\boldsymbol{D}|\boldsymbol{T}) = \int \mathcal{L}(\boldsymbol{D}|\boldsymbol{R}(\boldsymbol{T};\boldsymbol{\theta}_s),\boldsymbol{B}(\boldsymbol{\theta}_s,\boldsymbol{\theta}_b)) \cdot \mathcal{N}(\boldsymbol{\theta}_s) \cdot \mathcal{N}(\boldsymbol{\theta}_b)\, d\boldsymbol{\theta}_s\, d\boldsymbol{\theta}_b\,. \tag{7}$$

6.4 Binning optimization and asymmetry extraction

For each measurement, the choice of binning for the $\Delta|y|$ and $\Delta|\eta|$ distributions is optimized by minimizing the expected statistical uncertainty while allowing only a negligible bias in the linearity of the calibration curve. The optimal binnings are found to be 4 and 16 bins in an interval between -5 and 5 for the inclusive measurements of the $\Delta|y|$ and $\Delta|\eta|$ distributions, respectively. For the differential measurements, 4 bins are used for the $\Delta|y|$ and $\Delta|\eta|$ distributions for each of the chosen $m_{t\bar{t}}$, $p_{\mathrm{T,t\bar{t}}}$ and $\beta_{z,t\bar{t}}$ ranges. Due to the limited size of the data sample, only two ranges of values are considered for the $m_{t\bar{t}}$, $p_{\mathrm{T,t\bar{t}}}$ and $\beta_{z,t\bar{t}}$ variables. The charge asymmetry predicted in the SM is expected to increase as a function of $m_{t\bar{t}}$ while it is expected to be large for low $p_{\mathrm{T,t\bar{t}}}$ and small and roughly constant for higher $p_{\mathrm{T,t\bar{t}}}$. The exact boundary between the bins for $m_{t\bar{t}}$ was chosen to minimize the expected uncertainties in the bins. For $p_{\mathrm{T,t\bar{t}}}$, the boundary was set at 30 GeVas a compromise between the uncertainty optimization and the interest in the $p_{\mathrm{T,t\bar{t}}}$ dependence described above. For $\beta_{z,t\bar{t}}$, the boundary at 0.6 is motivated by the large difference of the predicted asymmetry between SM and BSM models in the range (0.6,1.0) [19]. Table 3 summarizes the differential bins used in the analysis.

For the optimized binning choice, more than 50% of the events populate the diagonal bins of the migration matrix for the $\Delta|y|$ distribution, and more than 97% for $\Delta|\eta|$. The rectangular migration matrix, normalized by row for each channel, used for the inclusive $t\bar{t}$ asymmetry measurement is shown in Fig. 3. Due to the nonuniform shape of the $\Delta|y|$ distribution, the matrix is not symmetric around the diagonal. The

Table 3: Bins and ranges used for the inclusive and differential measurements. The binning choices used in the $\Delta|\eta|$ and $\Delta|y|$ distributions are shown. The bins are symmetric around zero.

		$\Delta\|\eta\|$	$\Delta\|y\|$
Inclusive		[0.0, 0.3, 0.6, 0.9, 1.2, 1.5, 1.7, 1.9, 5.0]	[0.0, 0.75, 5.0]
$m_{t\bar{t}}$	0–500 GeV	[0.0, 0.8, 5.0]	[0.0, 0.6, 5.0]
	500–2000 GeV	[0.0, 1.4, 5.0]	[0.0, 1.2, 5.0]
$\beta_{t\bar{t}}$	0–0.6	[0.0, 0.8, 5.0]	[0.0, 0.5, 5.0]
	0.6–1.0	[0.0, 1.2, 5.0]	[0.0, 0.9, 5.0]
$p_{\mathrm{T}}^{t\bar{t}}$	0–30 GeV	[0.0, 0.7, 5.0]	[0.0, 0.8, 5.0]
	30–1000 GeV	[0.0, 0.7, 5.0]	[0.0, 0.8, 5.0]

migrations are symmetric around zero and do not affect the asymmetry value. The $\Delta|y|$ and $\Delta|\eta|$ input distributions used for the inclusive measurement are shown in Fig. 4.

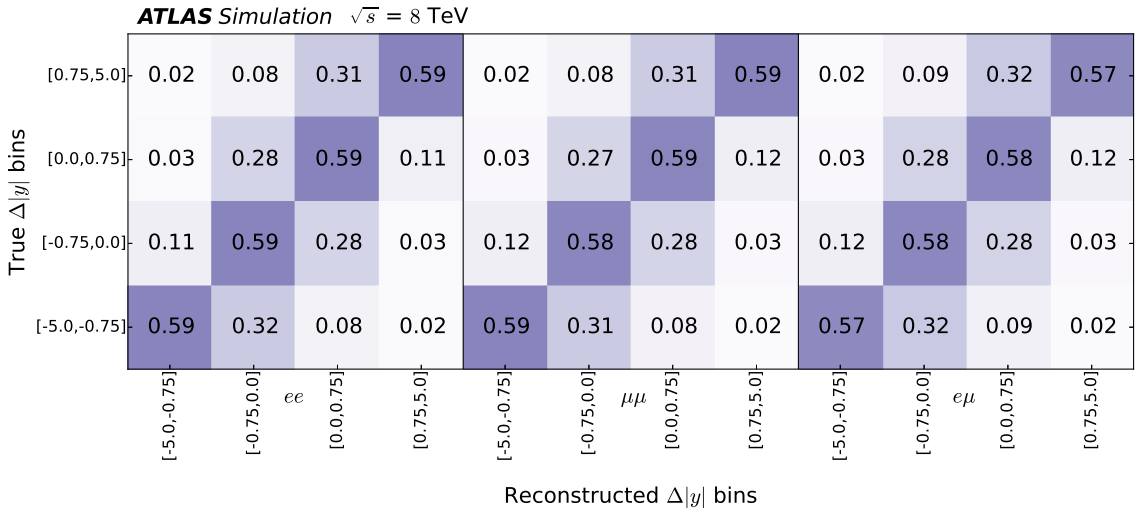

Figure 3: Rectangular migration matrix for the $\Delta|y|$ observable in the fiducial volume. The first four columns correspond to the *ee* channel, followed by $\mu\mu$ and $e\mu$. The numbers are normalized by row for each channel.

The asymmetry values are extracted by taking the mean of the posterior probability density obtained during the unfolding procedure. The uncertainty is obtained from the standard deviation of the posterior probability density.

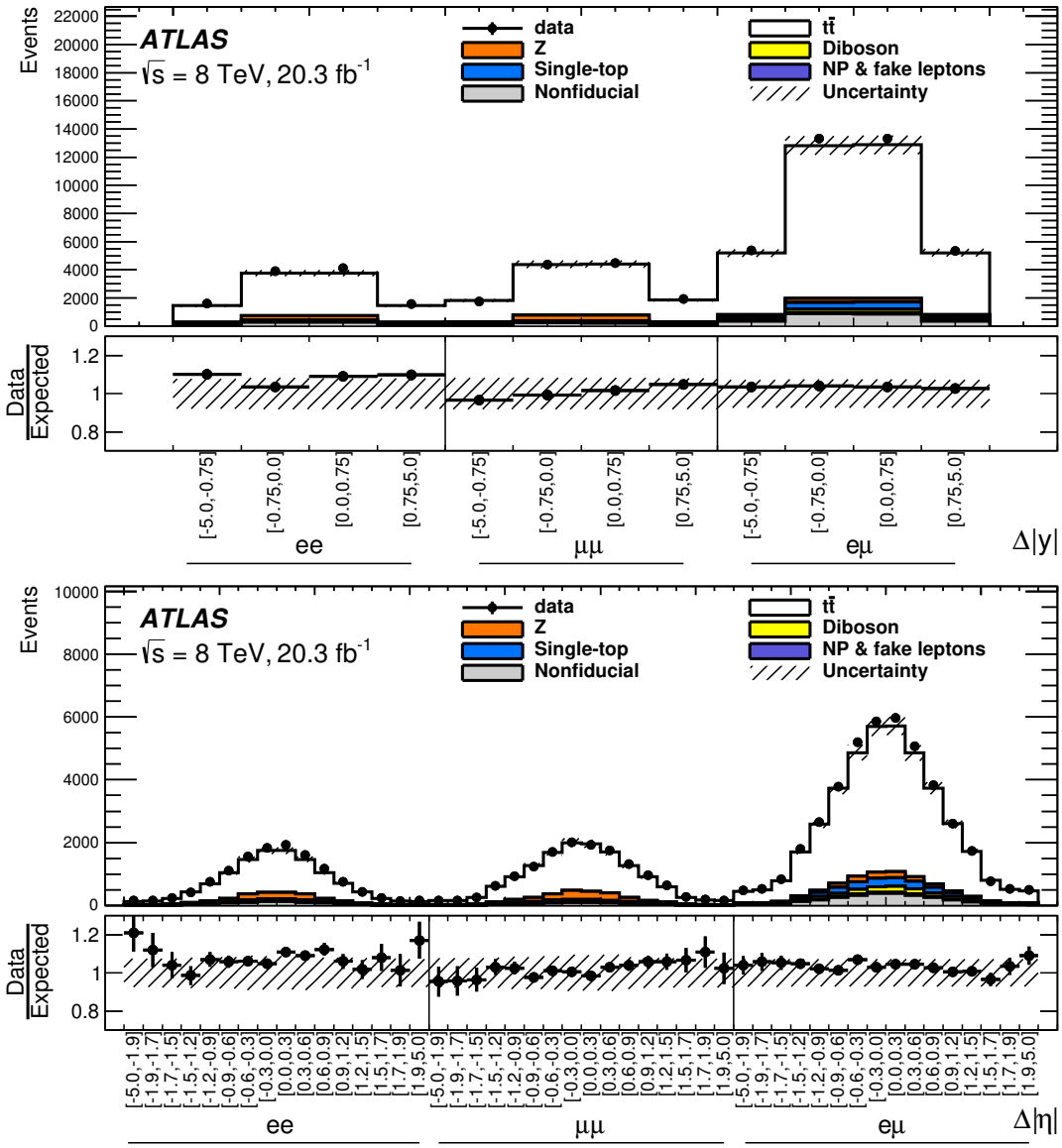

Figure 4: Input distributions for the inclusive $t\bar{t}$ (top) and leptonic (bottom) asymmetry measurements. The first 4 $\Delta|y|$ and 16 $\Delta|\eta|$ bins correspond to the ee channel, followed by $\mu\mu$ and $e\mu$. The bin boundaries are symmetric around zero and are defined as $[0.0, 0.75, 5.0]$ and $[0.0, 0.3, 0.6, 0.9, 1.2, 1.5, 1.7, 1.9, 5.0]$ for $\Delta|y|$ and $\Delta|\eta|$, respectively. The data/expected ratio is also shown.

7 Systematic uncertainties

Four classes of systematic uncertainties affect the measurement of the charge asymmetry: detector modeling uncertainties, uncertainties related to the estimation of the backgrounds, signal modeling uncertainties, and other uncertainties, which involve the top-quark reconstruction, the bias introduced by the unfolding procedure and the MC statistical uncertainty.

The first two categories are estimated within the unfolding through the marginalization procedure where

the total uncertainty includes these systematic uncertainties together with the statistical uncertainty. In order to estimate the impact of each source of systematic uncertainty, pseudodata corresponding to the sum of the nominal signal and background samples is used. The unfolding procedure with marginalization is applied to the pseudodata and constraints on the systematic uncertainties are obtained. These constraints are then used to build the $\pm 1\sigma$ variations of the prediction. The varied pseudodata are then unfolded without marginalization. The impact of each systematic uncertainty is computed by taking half of the difference between the results obtained from the $\pm 1\sigma$ variations of pseudodata. Clearly, this is only an approximate estimate of the individual contribution of each source of systematic uncertainty within the overall marginalization procedure.

The signal modeling uncertainties are not estimated through the marginalization procedure. For these uncertainties, the migration matrix is fixed to the nominal $t\bar{t}$ sample and distributions obtained with different generators and different injected asymmetries are unfolded. The unfolded asymmetries are compared with the injected asymmetries and the calibration curves are obtained. The slopes and offsets of the calibration curves are extrapolated to the measured value in data.

The final category of systematic uncertainties involves different estimation methods. The uncertainty related to the top-quark reconstruction is estimated on pseudodata by varying the starting point of the smearing procedure within the kinematic reconstruction and repeating the unfolding. The bias introduced by the unfolding procedure is estimated by propagating the residual slope and offset of the nominal calibration curve to the measured value. The MC statistical uncertainty is estimated by varying the nominal migration matrix within the MC statistical uncertainty and the unfolding procedure is repeated for each variation. All sources of systematic uncertainties are discussed below in detail.

7.1 Detector modeling uncertainties

Lepton-related uncertainties

The reconstruction and identification efficiencies of electrons and muons, as well as the efficiency of the triggers used to record the events, differ between data and simulation. Scale factors, and their uncertainties, are derived using tag-and-probe techniques on $Z \to \ell^+\ell^-(\ell = e, \mu)$ in data and in simulated samples to correct the simulation for these differences [58, 59, 71, 72]. Moreover, the accuracy of the lepton momentum scale and resolution in simulation is also checked using reconstructed distributions of the $Z \to \ell^+\ell^-$ and $J/\psi \to \ell^+\ell^-$ masses. In the case of electrons, E/p studies using $W \to e\nu$ events are also used. Small differences are observed between data and simulation. Corrections for the lepton energy scale and resolution, and their related uncertainties are considered [58, 59, 72]. The uncertainties are propagated through this analysis and represent a minor source of uncertainty in the measurements.

Jet-related uncertainties

The jet energy scale and its uncertainty are derived combining information from test-beam data, LHC collision data, and simulation [61]. The jet energy scale uncertainty is split into 22 uncorrelated sources that have different jet p_{T} and η dependencies and are treated independently in this analysis. The total jet energy scale uncertainty is one of the dominant uncertainties in $A_{\mathrm{C}}^{t\bar{t}}$ and in the differential measurements of $A_{\mathrm{C}}^{\ell\ell}$. The jet reconstruction efficiency is found to be about 0.2% lower in simulation than in data for jets below 30 GeV and consistent with data for higher jet p_T. All jet-related kinematic variables (including

the missing transverse momentum) are recomputed by removing randomly 0.2% of the jets with p_{T} below 30 GeV and the event selection is repeated. The efficiency for each jet to satisfy the JVF requirement is measured in $Z \to \ell^+\ell^-$ + 1-jet events in data and simulation [62]. The corresponding uncertainty is evaluated in the analysis by changing the nominal JVF cut value and repeating the analysis using the modified cut value. The uncertainty related to the jet energy resolution is estimated by smearing the energy of jets in simulation by the difference between the jet energy resolutions for data and simulation [73]. Finally, the efficiencies to tag jets from b- and c-quarks, light quarks, and gluons in simulation are corrected by p_T- and η-dependent data/MC scale factors [63, 74, 75]. The uncertainties in these scale factors are propagated to the measured value. The impact on the measurement of the jet reconstruction efficiency, jet vertex fraction, jet resolution, and jet tagging efficiency is minor.

Missing transverse momentum

The systematic uncertainties associated with the momenta and energies of reconstructed objects (leptons and jets) are also propagated to the $E_{\mathrm{T}}^{\mathrm{miss}}$ calculation. The $E_{\mathrm{T}}^{\mathrm{miss}}$ reconstruction also receives contributions from the presence of low-p_{T} jets and calorimeter cells not included in reconstructed objects ("soft terms"). The systematic uncertainty of the soft terms is evaluated using $Z \to \mu^+\mu^-$ events using methods similar to those used in Ref. [64]. The uncertainty has a negligible effect on the measured asymmetries.

7.2 Background-related uncertainties

The uncertainties in the single-top-quark and diboson backgrounds are about 7% and 5%, respectively. These correspond to the uncertainties in the theoretical cross sections used for the normalization of the MC simulated samples.

The uncertainty in the normalization of the fake-lepton background is evaluated by using various Monte Carlo simulations for each process contributing to this background and propagating the change into the number of expected events in the signal region. In the $\mu\mu$ channel, the uncertainty is obtained by comparing a purely data-driven method based on the measurement of the efficiencies for real and fake loose leptons, and the estimation used in this analysis. Following a Bayesian procedure assuming constant a priori probability for a non-negative number of events, the resulting total relative uncertainties are $^{+193\%}_{-47\%}$ in the ee, $^{+80\%}_{-53\%}$ in the $\mu\mu$, and $^{+49\%}_{-45\%}$ in the $e\mu$ channel, where the uncertainties correspond to the 68% central probability region.

In the case of the Drell–Yan events, the detector modeling systematic uncertainties described previously are propagated to the scale factors derived in the control region by recalculating them for all the systematic uncertainty variations. An additional uncertainty of 6% is estimated by varying the Z mass window of the control region used to obtain the scale factors and is added in quadrature to obtain the final uncertainty in these scale factors.

This category represents a minor source of uncertainty in the measurement.

7.3 Signal modeling uncertainties

The uncertainty due to the choice of MC generator is obtained by taking the full difference between the POWHEG-hvq and MC@NLO predictions, both interfaced with HERWIG, while the uncertainty from parton showering and hadronization is obtained by comparing POWHEG-hvq interfaced with either PYTHIA6 or HERWIG. These components are among the dominant uncertainties. The effect produced by the different amount of ISR and FSR in the events is estimated as half the difference between the asymmetries obtained from MC samples with more or less ISR/FSR. These samples are generated with POWHEG-hvq interfaced with PYTHIA6 for which the parameters of the generation were varied to span the ranges compatible with the results of measurements of $t\bar{t}$ production in association with jets [76]. Finally, PDF uncertainties are obtained by using the error sets of CT10, MWST2008 and NNPDF2.3, and following the prescriptions recommended by the PDF4LHC working group [39]. The impact of the last two uncertainties is small.

7.4 Other uncertainties

Top-quark kinematic reconstruction

There is an intrinsic uncertainty of the reconstruction method due to the randomness in the smearing procedure. If the smearing starts from a different point it could lead to a different solution. The uncertainty from this effect is computed by performing pseudoexperiments on MC events. For each event, the $t\bar{t}$ system is reconstructed multiple times varying the starting point of the smearing procedure. Then, for each variation the unfolding procedure is repeated and the standard deviation of the asymmetries obtained is taken as the uncertainty. This represents one of the major systematic uncertainties for the measurements, but it is still only half of the statistical uncertainty for most of them.

Nonclosure uncertainties

When the calibration curve for the nominal signal POWHEG-hvq sample is estimated a residual slope and a nonzero offset are observed. This bias, introduced by the unfolding procedure, is propagated to the measured values in the same way as for the signal modeling uncertainties. This source of uncertainty is negligible in all the measurements.

MC sample size

The uncertainty associated with the limited size of the nominal signal POWHEG-hvq sample is evaluated by performing pseudoexperiments on MC events. The migration matrix is varied within the MC statistical uncertainty and the unfolding procedure is repeated. The standard deviation of the obtained asymmetries is taken as the uncertainty. This uncertainty has a minor impact on the measurements.

7.5 Summary of systematic uncertainties

Tables 4 and 5 show how each category of uncertainty affects the measurements of the lepton and $t\bar{t}$ asymmetry, respectively. The statistical uncertainty gives the largest contribution to the measurement, followed by the reconstruction and the signal modeling uncertainties. The signal modeling uncertainties are enhanced in the differential measurements by the migrations between the differential bins across the different MC generators used for their estimation. The uncertainty obtained by the sum in quadrature of the individual systematic uncertainties is slightly larger than the total marginalized uncertainty in the measurements.

Table 4: Absolute uncertainties from the different sources affecting the leptonic asymmetry of the three channels combined in the fiducial and full phase space.

		Absolute uncertainties in $A_{\mathrm{C}}^{\ell\ell}$									
		Fiducial volume					Full phase space				
		Statistics	Detector	Bkg	Signal modeling	Other	Statistics	Detector	Bkg	Signal modeling	Other
	Inclusive	0.005	0.001	0.001	0.002	0.001	0.005	0.001	0.001	0.004	0.001
$m_{t\bar{t}}$	0–500 GeV	0.008	0.002	0.001	0.005	0.005	0.008	0.002	0.001	0.005	0.006
	500–2000 GeV	0.012	0.004	< 0.001	0.013	0.005	0.011	0.004	< 0.001	0.014	0.005
$\beta_{t\bar{t}}$	0–0.6	0.007	0.003	< 0.001	0.004	0.004	0.007	0.002	< 0.001	0.005	0.005
	0.6–1.0	0.010	0.005	0.001	0.005	0.004	0.010	0.003	0.001	0.006	0.004
$p_{\mathrm{T}}^{t\bar{t}}$	0–30 GeV	0.015	0.009	0.001	0.015	0.006	0.015	0.010	0.001	0.017	0.007
	30–1000 GeV	0.011	0.004	0.001	0.012	0.005	0.010	0.004	0.001	0.013	0.006

Table 5: Absolute uncertainties from the different sources affecting the $t\bar{t}$ asymmetry of the three channels combined in the fiducial and full phase space.

		Absolute uncertainties in $A_{\mathrm{C}}^{t\bar{t}}$									
		Fiducial volume					Full phase space				
		Statistics	Detector	Bkg	Signal modeling	Other	Statistics	Detector	Bkg	Signal modeling	Other
	Inclusive	0.013	0.008	< 0.001	0.007	0.007	0.011	0.006	< 0.001	0.008	0.006
$m_{t\bar{t}}$	0–500 GeV	0.030	0.024	0.001	0.016	0.021	0.028	0.021	0.002	0.018	0.020
	500–2000 GeV	0.018	0.007	< 0.001	0.015	0.009	0.015	0.006	< 0.001	0.016	0.008
$\beta_{t\bar{t}}$	0–0.6	0.023	0.021	0.002	0.014	0.018	0.023	0.019	0.002	0.015	0.017
	0.6–1.0	0.021	0.009	0.001	0.013	0.011	0.018	0.009	0.001	0.013	0.010
$p_{\mathrm{T}}^{t\bar{t}}$	0–30 GeV	0.035	0.019	0.003	0.018	0.020	0.031	0.015	0.004	0.019	0.017
	30–1000 GeV	0.027	0.015	0.003	0.018	0.017	0.025	0.013	0.003	0.014	0.015

8 Results

Figures 5 and 6 show the inclusive and differential results for the leptonic and $t\bar{t}$ charge asymmetry in the fiducial region and in the full phase space. All the results are compatible with the Standard Model predictions [23, 25–27]. Figure 7 shows the unfolded distributions of the $\Delta|\eta|$ and $\Delta|y|$ observables for the inclusive measurement in the fiducial volume. The distributions are compared with Monte Carlo predictions at NLO provided by POWHEG-hvq. The measured inclusive values in the full phase space are

$A_C^{\ell\ell} = 0.008 \pm 0.006$ and $A_C^{t\bar{t}} = 0.021 \pm 0.016$. They are in agreement with the Standard Model predictions $A_C^{\ell\ell} = 0.0064 \pm 0.0003$ and $A_C^{t\bar{t}} = 0.0111 \pm 0.0004$ [23]. The measurements are consistent with other LHC asymmetry measurements at 8 TeV [19–21].

The statistical uncertainty is in most cases the dominant contribution to the total uncertainty. The dominant systematic uncertainties across all the measurements are the signal modeling and the kinematic reconstruction uncertainty. The signal modeling uncertainties are reduced in most of the cases by performing the measurements in the fiducial region, since the extrapolation from detector acceptance to the full phase space is avoided. The statistical uncertainty is slightly larger in the fiducial region than in the full phase space; this is expected because some reconstructed events fail the fiducial requirements in the fiducial analysis.

Figure 8 compares the values of $A_C^{\ell\ell}$ and $A_C^{t\bar{t}}$ from the inclusive measurements in the full phase space to the SM predictions and two BSM models [77] compatible with the Tevatron results. Two BSM models with a new color-octet particle that is exchanged in the s-channel are considered. In the model with the light octet, the new particle's mass ($m = 250$ GeV) is below the $t\bar{t}$ production threshold and its width is assumed to be $\Gamma = 0.2m$. The model with the heavy octet uses an octet mass beyond current limits from direct searches at the LHC. The corrections to $t\bar{t}$ production are independent of the mass but instead depend on the ratio of coupling to mass, which is assumed to be $1\,\text{TeV}^{-1}$. The new particles in both BSM models would not be visible as resonances in the $m_{t\bar{t}}$ spectrum at the Tevatron or at the LHC. In the figures, model predictions for different left-handed, right-handed, and axial coupling constants to top quarks are shown. The ellipses correspond to the 1σ and 2σ total uncertainty in the measurements. The correlation between these two measurements is taken into account. The statistical and detector systematic uncertainty correlation between $A_C^{\ell\ell}$ and $A_C^{t\bar{t}}$ is found to be 30%. The modeling systematic uncertainties are assumed to be 100% correlated. The resulting correlation between $A_C^{\ell\ell}$ and $A_C^{t\bar{t}}$ is about 48%. The measurements are compatible with the SM and do not exclude the two sets of BSM models considered.

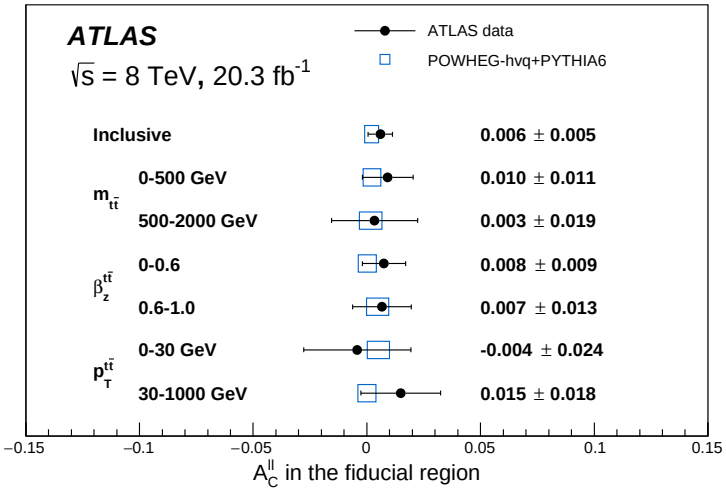

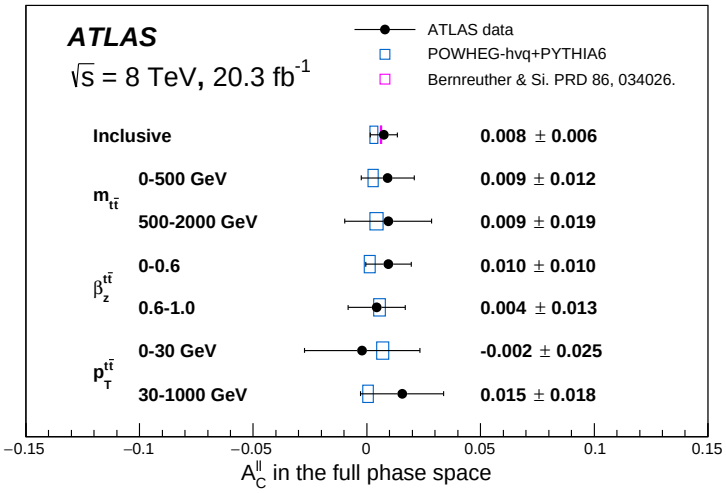

Figure 5: Summary of all the measurements in this paper for the leptonic asymmetry in the fiducial volume (top) and full phase space (bottom). The predictions shown in blue are obtained using POWHEG-hvq + PYTHIA6 at NLO where the uncertainties are statistical, and the corresponding theoretical uncertainties are small compared to the experimental precision. The inclusive measurement in the full phase space is compared to a NLO + EW prediction [23].

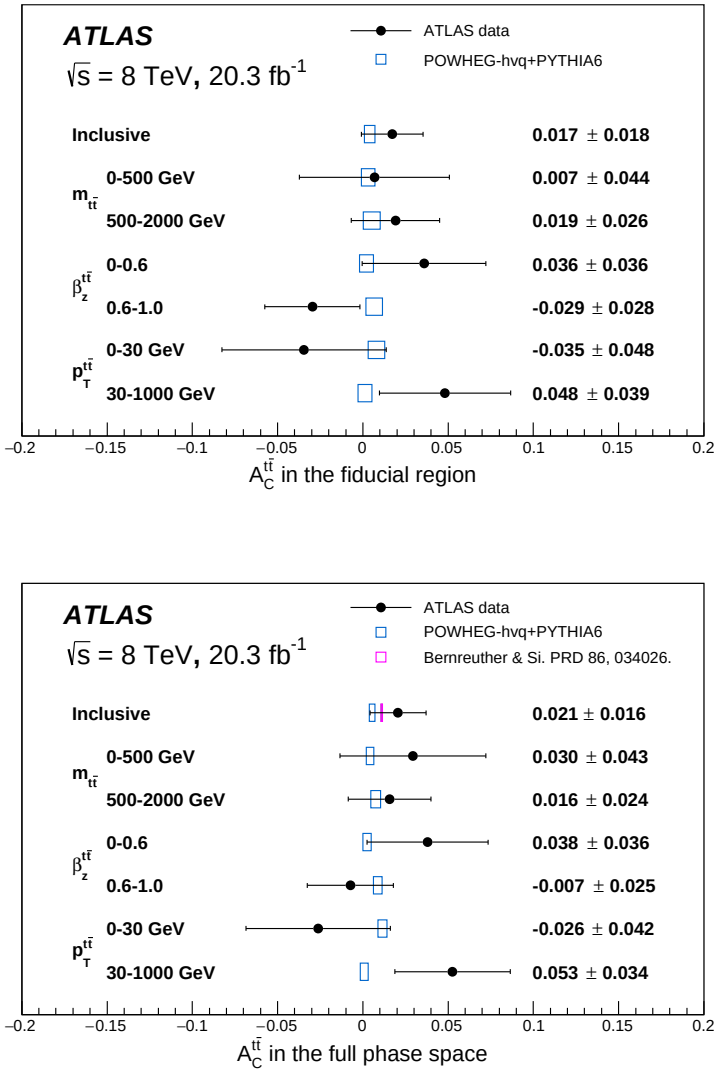

Figure 6: Summary of all the measurements in this paper for the $t\bar{t}$ asymmetry in the fiducial volume (top) and full phase space (bottom). The predictions shown in blue are obtained using POWHEG-hvq + PYTHIA6 at NLO where the uncertainties are statistical, and the corresponding theoretical uncertainties are small compared to the experimental precision. The inclusive measurement in the full phase space is compared to a NLO + EW prediction [23].

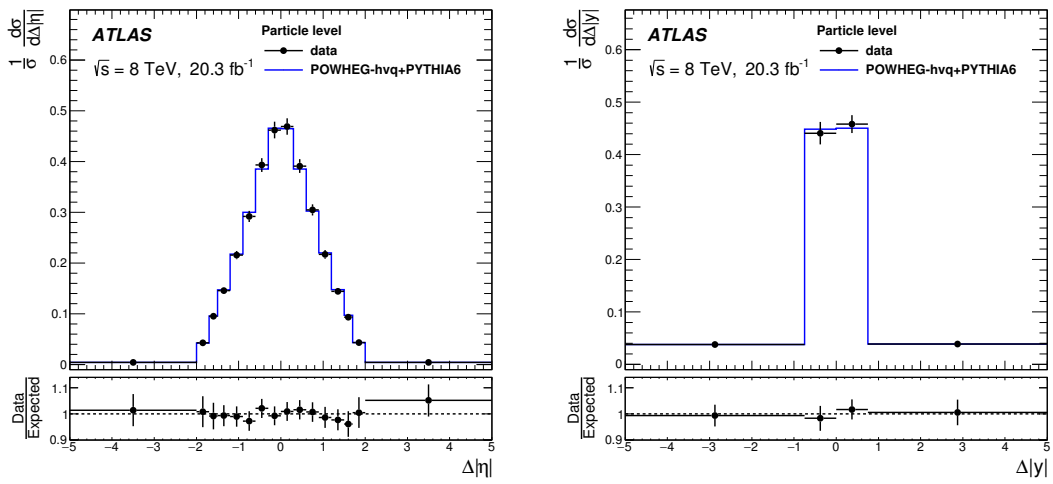

Figure 7: Data distribution after the unfolding procedure compared with the POWHEG-hvq + PYTHIA6 prediction at NLO for the inclusive $\Delta|\eta|$ (left) and $\Delta|y|$ (right) observables in the fiducial volume. The data/expected ratio is also shown.

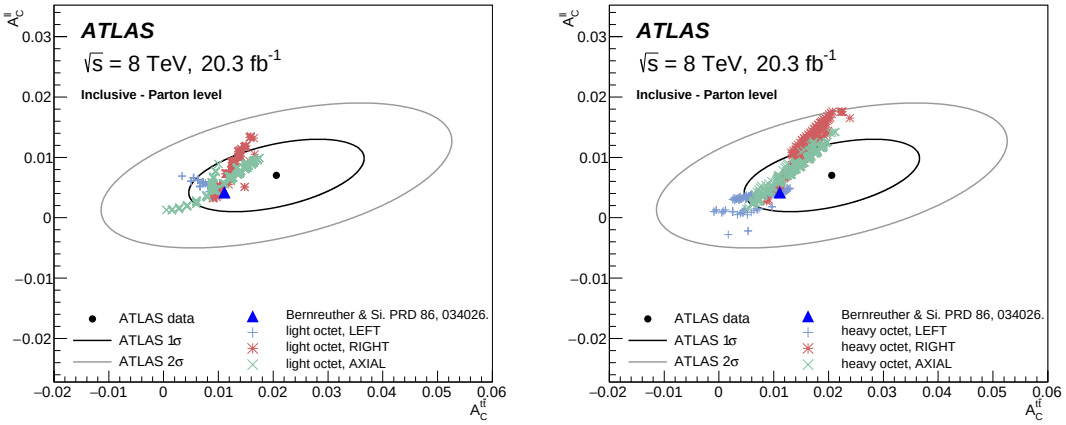

Figure 8: Comparison of the inclusive $A_{\mathrm{C}}^{\ell\ell}$ and $A_{\mathrm{C}}^{t\bar{t}}$ measurement values in the full phase space to the SM NLO QCD+EW prediction [23] and to two benchmark BSM models [77], one with a light octet with mass below the $t\bar{t}$ production threshold (left) and one with a heavy octet with mass beyond the reach of the LHC (right), for various couplings as described in the legend. Ellipses corresponding to 1σ and 2σ combined statistical and systematic uncertainties of the measurement, including the correlation between $A_{\mathrm{C}}^{\ell\ell}$ and $A_{\mathrm{C}}^{t\bar{t}}$, are also shown.

9 Conclusion

Measurements of the leptonic and $t\bar{t}$ charge asymmetry in the dilepton channel, characterized by two high-p_{T} leptons (electrons or muons), are presented. The measurements, corrected for detector resolution and acceptance effects, are performed using data corresponding to an integrated luminosity of 20.3 fb^{-1} of pp collisions at $\sqrt{s} = 8$ TeV collected by the ATLAS detector at the LHC. The inclusive asymmetries are measured in the full phase space to be:

$$A_{\mathrm{C}}^{\ell\ell} = 0.008 \pm 0.006 \text{ and}$$

$$A_{\mathrm{C}}^{t\bar{t}} = 0.021 \pm 0.016.$$

They are in agreement with the Standard Model predictions $A_{\mathrm{C}}^{\ell\ell} = 0.0064 \pm 0.0003$ and $A_{\mathrm{C}}^{t\bar{t}} = 0.0111 \pm 0.0004$. Differential measurements of the asymmetries as a function of the invariant mass, transverse momentum, and longitudinal boost of the $t\bar{t}$ system are also performed and they are found to be in agreement with the SM predictions, although they have relatively large uncertainties. All measurements are also performed in a fiducial region at particle level where the modeling uncertainties are reduced. For all measurements, the statistical uncertainty is the dominant contribution to the total uncertainty. The unfolded distributions of lepton $\Delta|\eta|$ and $t\bar{t}$ $\Delta|y|$ are provided. Good agreement between the corrected distributions and the predictions of Powheg-hvq + Pythia6 is observed.

Acknowledgments

We thank CERN for the very successful operation of the LHC, as well as the support staff from our institutions without whom ATLAS could not be operated efficiently.

We acknowledge the support of ANPCyT, Argentina; YerPhI, Armenia; ARC, Australia; BMWFW and FWF, Austria; ANAS, Azerbaijan; SSTC, Belarus; CNPq and FAPESP, Brazil; NSERC, NRC and CFI, Canada; CERN; CONICYT, Chile; CAS, MOST and NSFC, China; COLCIENCIAS, Colombia; MSMT CR, MPO CR and VSC CR, Czech Republic; DNRF and DNSRC, Denmark; IN2P3-CNRS, CEA-DSM/IRFU, France; GNSF, Georgia; BMBF, HGF, and MPG, Germany; GSRT, Greece; RGC, Hong Kong SAR, China; ISF, I-CORE and Benoziyo Center, Israel; INFN, Italy; MEXT and JSPS, Japan; CNRST, Morocco; FOM and NWO, Netherlands; RCN, Norway; MNiSW and NCN, Poland; FCT, Portugal; MNE/IFA, Romania; MES of Russia and NRC KI, Russian Federation; JINR; MESTD, Serbia; MSSR, Slovakia; ARRS and MIZŠ, Slovenia; DST/NRF, South Africa; MINECO, Spain; SRC and Wallenberg Foundation, Sweden; SERI, SNSF and Cantons of Bern and Geneva, Switzerland; MOST, Taiwan; TAEK, Turkey; STFC, United Kingdom; DOE and NSF, United States of America. In addition, individual groups and members have received support from BCKDF, the Canada Council, CANARIE, CRC, Compute Canada, FQRNT, and the Ontario Innovation Trust, Canada; EPLANET, ERC, FP7, Horizon 2020 and Marie Skłodowska-Curie Actions, European Union; Investissements d'Avenir Labex and Idex, ANR, Région Auvergne and Fondation Partager le Savoir, France; DFG and AvH Foundation, Germany; Herakleitos, Thales and Aristeia programmes co-financed by EU-ESF and the Greek NSRF; BSF, GIF and Minerva, Israel; BRF, Norway; Generalitat de Catalunya, Generalitat Valenciana, Spain; the Royal Society and Leverhulme Trust, United Kingdom.

The crucial computing support from all WLCG partners is acknowledged gratefully, in particular from CERN, the ATLAS Tier-1 facilities at TRIUMF (Canada), NDGF (Denmark, Norway, Sweden), CC-IN2P3 (France), KIT/GridKA (Germany), INFN-CNAF (Italy), NL-T1 (Netherlands), PIC (Spain), ASGC (Taiwan), RAL (UK) and BNL (USA), the Tier-2 facilities worldwide and large non-WLCG resource providers. Major contributors of computing resources are listed in Ref. [78].

References

[1] C. T. Hill, *Topcolor assisted technicolor*, Phys. Lett. B **345** (1995) 483–489.

[2] B. Lillie, L. Randall, and L.-T. Wang, *The Bulk RS KK-gluon at the LHC*, JHEP **09** (2007) 074.

[3] J. O.Antunano and G. Rodrigo, *Top quarks, axigluons and charge asymmetries at hadron colliders*, Phys. Rev. D **77** (2008) 014003.

[4] J. L. Rosner, *Prominent decay modes of a leptophobic Z'*, Phys. Lett. B **387** (1996) 113–117.

[5] P. Ferrario and G. Rodrigo, *Massive color-octet bosons and the charge asymmetries of top quarks at hadron colliders*, Phys. Rev. D **78** (2008) 094018.

[6] J. A. Aguilar-Saavedra et al., *Asymmetries in top quark pair production at hadron colliders*, Rev. Mod. Phys. **87** (2015) 421–455.

[7] T. Aaltonen et al., CDF Collaboration, *Forward-Backward Asymmetry in Top Quark Pair Production in $p\bar{p}$ collisions at $\sqrt{s} = 1.96$ TeV*, Phys. Rev. Lett. **101** (2008) 202001.

[8] T. Aaltonen et al., CDF Collaboration, *Evidence for a mass dependent forward-backward asymmetry in top quark pair production*, Phys. Rev. D **83** (2011) 112003.

[9] T. Aaltonen et al., CDF Collaboration, *Measurement of the top quark forward-backward production asymmetry and its dependence on event kinematic properties*, Phys. Rev. D **87** (2013) 092002.

[10] V. M. Abazov et al., D0 Collaboration, *Measurements of the Forward-Backward Charge Asymmetry in Top-Quark Pair Production*, Phys. Rev. Lett. **100** (2008) 142002.

[11] V. M. Abazov et al., D0 Collaboration, *Measurement of the forward-backward asymmetry in top quark-antiquark production in $p\overline{p}$ collisions using the* lepton+jets *channel*, Phys. Rev. D **90** (2014) 072011.

[12] V. M. Abazov et al., D0 Collaboration, *Simultaneous measurement of forward-backward asymmetry and top polarization in dilepton final states from $t\bar{t}$ production at the Tevatron*, Phys. Rev. D **92** (2015) 052007.

[13] M. Czakon, P. Fiedler, and A. Mitov, *Resolving the Tevatron Top Quark Forward-Backward Asymmetry Puzzle: Fully Differential Next-to-Next-to-Leading-Order Calculation*, Phys. Rev. Lett. **115** (2015) 052001.

[14] J. H. Kühn and G. Rodrigo, *Charge asymmetry in hadroproduction of heavy quarks*, Phys. Rev. Lett. **81** (1998) 49–52.

[15] ATLAS Collaboration, *Measurement of the charge asymmetry in dileptonic decays of top quark pairs in pp collisions at $\sqrt{s} = 7$ TeV using the ATLAS detector*, JHEP **05** (2015) 061.

[16] ATLAS Collaboration, *Measurement of the charge asymmetry in top quark pair production in pp collisions at $\sqrt{s} = 7$ TeV using the ATLAS detector*, Eur. Phys. J. C **72** (2012) 2039.

[17] CMS Collaboration, *Inclusive and differential measurements of the $t\bar{t}$ charge asymmetry in proton-proton collisions at 7 TeV*, Phys. Lett. B **717** (2012) 129–150.

[18] CMS Collaboration, *Measurements of the $t\bar{t}$ charge asymmetry using the dilepton decay channel in pp collisions at $\sqrt{s}$ = 7 TeV*, JHEP **04** (2014) 191.

[19] ATLAS Collaboration, *Measurement of the charge asymmetry in top-quark pair production in the lepton-plus-jets final state in pp collision data at $\sqrt{s}$ = 8 TeV with the ATLAS detector*, Eur. Phys. J. C **76** (2016) 87.

[20] CMS Collaboration, *Inclusive and differential measurements of the $t\bar{t}$ charge asymmetry in pp collisions at $\sqrt{s}$ = 8 TeV*, Phys. Lett. B **757** (2016) 154–179.

[21] CMS Collaboration, *Measurement of the charge asymmetry in top quark pair production in pp collisions at $\sqrt{s}$ = 8 TeV using a template method*, Phys. Rev. D **93** (2016) 034014.

[22] CMS Collaboration, *Measurements of t t-bar charge asymmetry using dilepton final states in pp collisions at $\sqrt{s}$ = 8 TeV*, (2016), arXiv:1603.06221 [hep-ex].

[23] W. Bernreuther and Z.-G. Si, *Top quark and leptonic charge asymmetries for the Tevatron and LHC*, Phys. Rev. D **86** (2012) 034026.

[24] ATLAS Collaboration, *The ATLAS Experiment at the CERN Large Hadron Collider*, JINST **3** (2008) S08003.

[25] S. Alioli et al., *A general framework for implementing NLO calculations in shower Monte Carlo programs: the POWHEG BOX*, JHEP **06** (2010) 043.

[26] S. Frixione, P. Nason, and C. Oleari, *Matching NLO QCD computations with Parton Shower simulations: the POWHEG method*, JHEP **11** (2007) 070.

[27] P. Nason, *A New method for combining NLO QCD with shower Monte Carlo algorithms*, JHEP **11** (2004) 040.

[28] H.-L. Lai et al., *New parton distributions for collider physics*, Phys. Rev. D **82** (2010) 074024.

[29] T. Sjöstrand, S. Mrenna, and P. Z. Skands, *PYTHIA 6.4 Physics and Manual*, JHEP **05** (2006) 026.

[30] J. Pumplin et al., *New generation of parton distributions with uncertainties from global QCD analysis*, JHEP **07** (2002) 012.

[31] P. Z. Skands, *Tuning Monte Carlo Generators: The Perugia Tunes*, Phys. Rev. D **82** (2010) 074018.

[32] M. Cacciari et al., *Top-pair production at hadron colliders with next-to-next-to-leading logarithmic soft-gluon resummation*, Phys. Lett. B **710** (2012) 612–622.

[33] M. Beneke et al., *Hadronic top-quark pair production with NNLL threshold resummation*, Nucl. Phys. B **855** (2012) 695–741.

[34] P. Baernreuther, M. Czakon, and A. Mitov, *Percent Level Precision Physics at the Tevatron: First Genuine NNLO QCD Corrections to $q\bar{q} \to t\bar{t} + X$*, Phys. Rev. Lett. **109** (2012) 132001.

[35] M. Czakon and A. Mitov, *NNLO corrections to top-pair production at hadron colliders: the all-fermionic scattering channels*, JHEP **12** (2012) 054.

[36] M. Czakon and A. Mitov, *NNLO corrections to top pair production at hadron colliders: the quark-gluon reaction*, JHEP **13** (2013) 080.

[37] M. Czakon, P. Fiedler, and A. Mitov, *Total Top-Quark Pair-Production Cross Section at Hadron Colliders Through $O(\alpha_S^4)$*, Phys. Rev. Lett. **110** (2013) 252004.

[38] M. Czakon and A. Mitov, *Top++: A Program for the Calculation of the Top-Pair Cross-Section at Hadron Colliders*, Comput. Phys. Commun. **185** (2014) 2930.

[39] M. Botje et al., *The PDF4LHC Working Group Interim Recommendations*, (2011).

[40] A. D. Martin et al., *Parton distributions for the LHC*, Eur. Phys. J. C **63** (2009) 189–285.

[41] A. D. Martin et al., *Uncertainties on alpha(S) in global PDF analyses and implications for predicted hadronic cross sections*, Eur. Phys. J. C **64** (2009) 653–680.

[42] H.-L. Lai et al., *New parton distributions for collider physics*, Phys. Rev. D **82** (2010) 074024.

[43] J. Gao et al., *The CT10 NNLO Global Analysis of QCD*, Phys. Rev. D **89** (2014) 033009.

[44] R. D. Ball et al., *Parton distributions with LHC data*, Nucl. Phys. B **867** (2013) 244–289.

[45] N. Kidonakis, *Two-loop soft anomalous dimensions for single top quark associated production with a W- or H-*, Phys. Rev. D **82** (2010) 054018.

[46] M. L. Mangano et al., *ALPGEN, a generator for hard multiparton processes in hadronic collisions*, JHEP **07** (2003) 001.

[47] G. Corcella et al., *HERWIG 6: An Event generator for hadron emission reactions with interfering gluons (including supersymmetric processes)*, JHEP **01** (2001) 010.

[48] J. M. Butterworth and M. H. Seymour, *JIMMY4: Multiparton Interactions in Herwig for the LHC*, http://projects.hepforge.org/jimmy/, 2004, URL: http://projects.hepforge.org/jimmy/.

[49] M. L. Mangano, M. Moretti, and R. Pittau, *Multijet matrix elements and shower evolution in hadronic collisions: $Wb\bar{b}$ + n jets as a case study*, Nucl. Phys. B **632** (2002) 343–362.

[50] J. Alwall et al., *MadGraph 5 : Going Beyond*, JHEP **06** (2011) 128.

[51] T. Sjöstrand, S. Mrenna, and P. Z. Skands, *A Brief Introduction to PYTHIA 8.1*, Comput. Phys. Commun. **178** (2008) 852–867.

[52] J. M. Campbell and R. K. Ellis, *An Update on vector boson pair production at hadron colliders*, Phys. Rev. D **60** (1999) 113006.

[53] J. M. Campbell and R. K. Ellis, *$t\bar{t}W^{+-}$ production and decay at NLO*, JHEP **07** (2012) 052.

[54] M. V. Garzelli et al., *$t\ \bar{t}\ W^{+-}$ and $t\ \bar{t}\ Z$ Hadroproduction at NLO accuracy in QCD with Parton Shower and Hadronization effects*, JHEP **11** (2012) 056.

[55] ATLAS Collaboration, *The ATLAS Simulation Infrastructure*, Eur. Phys. J. C **70** (2010) 823–874.

[56] S. Agostinelli et al., *GEANT4: A simulation toolkit*, Nucl. Instrum. Meth. A **506** (2003) 250–303.

[57] ATLAS Collaboration, "The simulation principle and performance of the ATLAS fast calorimeter simulation FastCaloSim," ATL-PHYS-PUB-2010-013, 2010, URL: http://cds.cern.ch/record/1300517.

[58] ATLAS Collaboration, *Electron reconstruction and identification efficiency measurements with the ATLAS detector using the 2011 LHC proton-proton collision data*, Eur. Phys. J. C **74** (2014) 2941.

[59] ATLAS Collaboration, *Measurement of the muon reconstruction performance of the ATLAS detector using 2011 and 2012 LHC proton–proton collision data*, Eur. Phys. J. C **74** (2014) 3130.

[60] M. Cacciari, G. P. Salam, and G. Soyez, *The anti−k_t jet clustering algorithm*, JHEP **04** (2008) 063.

[61] ATLAS Collaboration, *Jet energy measurement and its systematic uncertainty in proton-proton collisions at $\sqrt{s}$ = 7 TeV with the ATLAS detector*, Eur. Phys. J. C **75** (2015) 17.

[62] ATLAS Collaboration, *Performance of pile-up mitigation techniques for jets in pp collisions at $\sqrt{s}$ = 8 TeV using the ATLAS detector*, (2015), arXiv:1510.03823 [hep-ex].

[63] ATLAS Collaboration, *Performance of b-Jet Identification in the ATLAS Experiment*, JINST **11** (2016) P04008.

[64] ATLAS Collaboration, *Performance of Missing Transverse Momentum Reconstruction in Proton-Proton Collisions at $\sqrt{s}$ = 7 TeV with ATLAS*, Eur. Phys. J. C **72** (2012) 1844.

[65] A. Abulencia et al., CDF Collaboration, *Measurement of the top quark mass using template methods on dilepton events in p anti-p collisions at $\sqrt{s}$ = 1.96 TeV*, Phys. Rev. D **73** (2006) 112006.

[66] T. Aaltonen et al., CDF Collaboration, *W boson polarization measurement in the $t\bar{t}$ dilepton channel using the CDF II Detector*, Phys. Lett. B **722** (2013) 48–54.

[67] M. Cacciari, G. P. Salam, and G. Soyez, *The Catchment Area of Jets*, JHEP **04** (2008) 005.

[68] ATLAS Collaboration, *Differential top-antitop cross-section measurements as a function of observables constructed from final-state particles using pp collisions at $\sqrt{s}$ = 7 TeV in the ATLAS detector*, JHEP **06** (2015) 100.

[69] G. Choudalakis, *Fully Bayesian Unfolding*, (2012), arXiv:1201.4612 [hep-ex].

[70] J. A. Aguilar-Saavedra, *Identifying top partners at LHC*, JHEP **11** (2009) 030.

[71] ATLAS Collaboration, *Performance of the ATLAS Trigger System in 2010*, Eur. Phys. J. C **72** (2012) 1849.

[72] ATLAS Collaboration, *Electron and photon energy calibration with the ATLAS detector using LHC Run 1 data*, Eur. Phys. J. C **74** (2014) 3071.

[73] ATLAS Collaboration, *Jet energy resolution in proton-proton collisions at $\sqrt{s}$ = 7 TeV recorded in 2010 with the ATLAS detector*, Eur. Phys. J. C **73** (2013) 2306.

[74] ATLAS Collaboration, "Calibration of *b*-tagging using dileptonic top pair events in a combinatorial likelihood approach with the ATLAS experiment," ATLAS-CONF-2014-004, https://cds.cern.ch/record/1664335.

[75] ATLAS Collaboration, "Calibration of the performance of *b*-tagging for *c* and light-flavour jets in the 2012 ATLAS data," ATLAS-CONF-2014-046, https://cds.cern.ch/record/1741020.

[76] ATLAS Collaboration, *Measurement of $t\bar{t}$ production with a veto on additional central jet activity in pp collisions at $\sqrt{s}$ = 7 TeV using the ATLAS detector*, Eur. Phys. J. C **72** (2012) 2043.

[77] J. A. Aguilar-Saavedra, *Portrait of a colour octet*, JHEP **08** (2014) 172.

[78] ATLAS Collaboration, *ATLAS Computing Acknowledgements 2016-2017*, ATL-GEN-PUB-2016-002, 2016, URL: http://cds.cern.ch/record/2202407.

The ATLAS Collaboration

G. Aad[87], B. Abbott[114], J. Abdallah[65], O. Abdinov[12], B. Abeloos[118], R. Aben[108], M. Abolins[92], O.S. AbouZeid[138], N.L. Abraham[150], H. Abramowicz[154], H. Abreu[153], R. Abreu[117], Y. Abulaiti[147a,147b], B.S. Acharya[164a,164b,a], L. Adamczyk[40a], D.L. Adams[27], J. Adelman[109], S. Adomeit[101], T. Adye[132], A.A. Affolder[76], T. Agatonovic-Jovin[14], J. Agricola[56], J.A. Aguilar-Saavedra[127a,127f], S.P. Ahlen[24], F. Ahmadov[67,b], G. Aielli[134a,134b], H. Akerstedt[147a,147b], T.P.A. Åkesson[83], A.V. Akimov[97], G.L. Alberghi[22a,22b], J. Albert[169], S. Albrand[57], M.J. Alconada Verzini[73], M. Aleksa[32], I.N. Aleksandrov[67], C. Alexa[28b], G. Alexander[154], T. Alexopoulos[10], M. Alhroob[114], M. Aliev[75a,75b], G. Alimonti[93a], J. Alison[33], S.P. Alkire[37], B.M.M. Allbrooke[150], B.W. Allen[117], P.P. Allport[19], A. Aloisio[105a,105b], A. Alonso[38], F. Alonso[73], C. Alpigiani[139], B. Alvarez Gonzalez[32], D. Álvarez Piqueras[167], M.G. Alviggi[105a,105b], B.T. Amadio[16], K. Amako[68], Y. Amaral Coutinho[26a], C. Amelung[25], D. Amidei[91], S.P. Amor Dos Santos[127a,127c], A. Amorim[127a,127b], S. Amoroso[32], N. Amram[154], G. Amundsen[25], C. Anastopoulos[140], L.S. Ancu[51], N. Andari[109], T. Andeen[11], C.F. Anders[60b], G. Anders[32], J.K. Anders[76], K.J. Anderson[33], A. Andreazza[93a,93b], V. Andrei[60a], S. Angelidakis[9], I. Angelozzi[108], P. Anger[46], A. Angerami[37], F. Anghinolfi[32], A.V. Anisenkov[110,c], N. Anjos[13], A. Annovi[125a,125b], M. Antonelli[49], A. Antonov[99], J. Antos[145b], F. Anulli[133a], M. Aoki[68], L. Aperio Bella[19], G. Arabidze[92], Y. Arai[68], J.P. Araque[127a], A.T.H. Arce[47], F.A. Arduh[73], J-F. Arguin[96], S. Argyropoulos[65], M. Arik[20a], A.J. Armbruster[32], L.J. Armitage[78], O. Arnaez[32], H. Arnold[50], M. Arratia[30], O. Arslan[23], A. Artamonov[98], G. Artoni[121], S. Artz[85], S. Asai[156], N. Asbah[44], A. Ashkenazi[154], B. Åsman[147a,147b], L. Asquith[150], K. Assamagan[27], R. Astalos[145a], M. Atkinson[166], N.B. Atlay[142], K. Augsten[129], G. Avolio[32], B. Axen[16], M.K. Ayoub[118], G. Azuelos[96,d], M.A. Baak[32], A.E. Baas[60a], M.J. Baca[19], H. Bachacou[137], K. Bachas[75a,75b], M. Backes[32], M. Backhaus[32], P. Bagiacchi[133a,133b], P. Bagnaia[133a,133b], Y. Bai[35a], J.T. Baines[132], O.K. Baker[176], E.M. Baldin[110,c], P. Balek[130], T. Balestri[149], F. Balli[137], W.K. Balunas[123], E. Banas[41], Sw. Banerjee[173,e], A.A.E. Bannoura[175], L. Barak[32], E.L. Barberio[90], D. Barberis[52a,52b], M. Barbero[87], T. Barillari[102], T. Barklow[144], N. Barlow[30], S.L. Barnes[86], B.M. Barnett[132], R.M. Barnett[16], Z. Barnovska[5], A. Baroncelli[135a], G. Barone[25], A.J. Barr[121], L. Barranco Navarro[167], F. Barreiro[84], J. Barreiro Guimarães da Costa[35a], R. Bartoldus[144], A.E. Barton[74], P. Bartos[145a], A. Basalaev[124], A. Bassalat[118], A. Basye[166], R.L. Bates[55], S.J. Batista[159], J.R. Batley[30], M. Battaglia[138], M. Bauce[133a,133b], F. Bauer[137], H.S. Bawa[144,f], J.B. Beacham[112], M.D. Beattie[74], T. Beau[82], P.H. Beauchemin[162], P. Bechtle[23], H.P. Beck[18,g], K. Becker[121], M. Becker[85], M. Beckingham[170], C. Becot[111], A.J. Beddall[20e], A. Beddall[20b], V.A. Bednyakov[67], M. Bedognetti[108], C.P. Bee[149], L.J. Beemster[108], T.A. Beermann[32], M. Begel[27], J.K. Behr[44], C. Belanger-Champagne[89], A.S. Bell[80], G. Bella[154], L. Bellagamba[22a], A. Bellerive[31], M. Bellomo[88], K. Belotskiy[99], O. Beltramello[32], N.L. Belyaev[99], O. Benary[154], D. Benchekroun[136a], M. Bender[101], K. Bendtz[147a,147b], N. Benekos[10], Y. Benhammou[154], E. Benhar Noccioli[176], J. Benitez[65], J.A. Benitez Garcia[160b], D.P. Benjamin[47], J.R. Bensinger[25], S. Bentvelsen[108], L. Beresford[121], M. Beretta[49], D. Berge[108], E. Bergeaas Kuutmann[165], N. Berger[5], F. Berghaus[169], J. Beringer[16], S. Berlendis[57], N.R. Bernard[88], C. Bernius[111], F.U. Bernlochner[23], T. Berry[79], P. Berta[130], C. Bertella[85], G. Bertoli[147a,147b], F. Bertolucci[125a,125b], I.A. Bertram[74], C. Bertsche[114], D. Bertsche[114], G.J. Besjes[38], O. Bessidskaia Bylund[147a,147b], M. Bessner[44], N. Besson[137], C. Betancourt[50], S. Bethke[102], A.J. Bevan[78], W. Bhimji[16], R.M. Bianchi[126], L. Bianchini[25], M. Bianco[32], O. Biebel[101], D. Biedermann[17], R. Bielski[86], N.V. Biesuz[125a,125b], M. Biglietti[135a], J. Bilbao De Mendizabal[51], H. Bilokon[49], M. Bindi[56], S. Binet[118], A. Bingul[20b], C. Bini[133a,133b], S. Biondi[22a,22b], D.M. Bjergaard[47], C.W. Black[151], J.E. Black[144], K.M. Black[24], D. Blackburn[139], R.E. Blair[6], J.-B. Blanchard[137],

J.E. Blanco[79], T. Blazek[145a], I. Bloch[44], C. Blocker[25], W. Blum[85,*], U. Blumenschein[56], S. Blunier[34a], G.J. Bobbink[108], V.S. Bobrovnikov[110,c], S.S. Bocchetta[83], A. Bocci[47], C. Bock[101], M. Boehler[50], D. Boerner[175], J.A. Bogaerts[32], D. Bogavac[14], A.G. Bogdanchikov[110], C. Bohm[147a], V. Boisvert[79], T. Bold[40a], V. Boldea[28b], A.S. Boldyrev[164a,164c], M. Bomben[82], M. Bona[78], M. Boonekamp[137], A. Borisov[131], G. Borissov[74], J. Bortfeldt[101], D. Bortoletto[121], V. Bortolotto[62a,62b,62c], K. Bos[108], D. Boscherini[22a], M. Bosman[13], J.D. Bossio Sola[29], J. Boudreau[126], J. Bouffard[2], E.V. Bouhova-Thacker[74], D. Boumediene[36], C. Bourdarios[118], S.K. Boutle[55], A. Boveia[32], J. Boyd[32], I.R. Boyko[67], J. Bracinik[19], A. Brandt[8], G. Brandt[56], O. Brandt[60a], U. Bratzler[157], B. Brau[88], J.E. Brau[117], H.M. Braun[175,*], W.D. Breaden Madden[55], K. Brendlinger[123], A.J. Brennan[90], L. Brenner[108], R. Brenner[165], S. Bressler[172], T.M. Bristow[48], D. Britton[55], D. Britzger[44], F.M. Brochu[30], I. Brock[23], R. Brock[92], G. Brooijmans[37], T. Brooks[79], W.K. Brooks[34b], J. Brosamer[16], E. Brost[117], J.H Broughton[19], P.A. Bruckman de Renstrom[41], D. Bruncko[145b], R. Bruneliere[50], A. Bruni[22a], G. Bruni[22a], BH Brunt[30], M. Bruschi[22a], N. Bruscino[23], P. Bryant[33], L. Bryngemark[83], T. Buanes[15], Q. Buat[143], P. Buchholz[142], A.G. Buckley[55], I.A. Budagov[67], F. Buehrer[50], M.K. Bugge[120], O. Bulekov[99], D. Bullock[8], H. Burckhart[32], S. Burdin[76], C.D. Burgard[50], B. Burghgrave[109], K. Burka[41], S. Burke[132], I. Burmeister[45], E. Busato[36], D. Büscher[50], V. Büscher[85], P. Bussey[55], J.M. Butler[24], A.I. Butt[3], C.M. Buttar[55], J.M. Butterworth[80], P. Butti[108], W. Buttinger[27], A. Buzatu[55], A.R. Buzykaev[110,c], S. Cabrera Urbán[167], D. Caforio[129], V.M. Cairo[39a,39b], O. Cakir[4a], N. Calace[51], P. Calafiura[16], A. Calandri[87], G. Calderini[82], P. Calfayan[101], L.P. Caloba[26a], D. Calvet[36], S. Calvet[36], T.P. Calvet[87], R. Camacho Toro[33], S. Camarda[32], P. Camarri[134a,134b], D. Cameron[120], R. Caminal Armadans[166], C. Camincher[57], S. Campana[32], M. Campanelli[80], A. Campoverde[149], V. Canale[105a,105b], A. Canepa[160a], M. Cano Bret[35e], J. Cantero[84], R. Cantrill[127a], T. Cao[42], M.D.M. Capeans Garrido[32], I. Caprini[28b], M. Caprini[28b], M. Capua[39a,39b], R. Caputo[85], R.M. Carbone[37], R. Cardarelli[134a], F. Cardillo[50], I. Carli[130], T. Carli[32], G. Carlino[105a], L. Carminati[93a,93b], S. Caron[107], E. Carquin[34b], G.D. Carrillo-Montoya[32], J.R. Carter[30], J. Carvalho[127a,127c], D. Casadei[19], M.P. Casado[13,h], M. Casolino[13], D.W. Casper[163], E. Castaneda-Miranda[146a], A. Castelli[108], V. Castillo Gimenez[167], N.F. Castro[127a,i], A. Catinaccio[32], J.R. Catmore[120], A. Cattai[32], J. Caudron[85], V. Cavaliere[166], E. Cavallaro[13], D. Cavalli[93a], M. Cavalli-Sforza[13], V. Cavasinni[125a,125b], F. Ceradini[135a,135b], L. Cerda Alberich[167], B.C. Cerio[47], A.S. Cerqueira[26b], A. Cerri[150], L. Cerrito[78], F. Cerutti[16], M. Cerv[32], A. Cervelli[18], S.A. Cetin[20d], A. Chafaq[136a], D. Chakraborty[109], S.K. Chan[59], Y.L. Chan[62a], P. Chang[166], J.D. Chapman[30], D.G. Charlton[19], A. Chatterjee[51], C.C. Chau[159], C.A. Chavez Barajas[150], S. Che[112], S. Cheatham[74], A. Chegwidden[92], S. Chekanov[6], S.V. Chekulaev[160a], G.A. Chelkov[67,j], M.A. Chelstowska[91], C. Chen[66], H. Chen[27], K. Chen[149], S. Chen[35c], S. Chen[156], X. Chen[35f], Y. Chen[69], H.C. Cheng[91], H.J Cheng[35a], Y. Cheng[33], A. Cheplakov[67], E. Cheremushkina[131], R. Cherkaoui El Moursli[136e], V. Chernyatin[27,*], E. Cheu[7], L. Chevalier[137], V. Chiarella[49], G. Chiarelli[125a,125b], G. Chiodini[75a], A.S. Chisholm[19], A. Chitan[28b], M.V. Chizhov[67], K. Choi[63], A.R. Chomont[36], S. Chouridou[9], B.K.B. Chow[101], V. Christodoulou[80], D. Chromek-Burckhart[32], J. Chudoba[128], A.J. Chuinard[89], J.J. Chwastowski[41], L. Chytka[116], G. Ciapetti[133a,133b], A.K. Ciftci[4a], D. Cinca[55], V. Cindro[77], I.A. Cioara[23], A. Ciocio[16], F. Cirotto[105a,105b], Z.H. Citron[172], M. Ciubancan[28b], A. Clark[51], B.L. Clark[59], M.R. Clark[37], P.J. Clark[48], R.N. Clarke[16], C. Clement[147a,147b], Y. Coadou[87], M. Cobal[164a,164c], A. Coccaro[51], J. Cochran[66], L. Coffey[25], L. Colasurdo[107], B. Cole[37], S. Cole[109], A.P. Colijn[108], J. Collot[57], T. Colombo[32], G. Compostella[102], P. Conde Muiño[127a,127b], E. Coniavitis[50], S.H. Connell[146b], I.A. Connelly[79], V. Consorti[50], S. Constantinescu[28b], C. Conta[122a,122b], G. Conti[32], F. Conventi[105a,k], M. Cooke[16], B.D. Cooper[80], A.M. Cooper-Sarkar[121], T. Cornelissen[175], M. Corradi[133a,133b], F. Corriveau[89,l], A. Corso-Radu[163], A. Cortes-Gonzalez[13], G. Cortiana[102], G. Costa[93a], M.J. Costa[167], D. Costanzo[140], G. Cottin[30], G. Cowan[79], B.E. Cox[86], K. Cranmer[111], S.J. Crawley[55], G. Cree[31], S. Crépé-Renaudin[57], F. Crescioli[82],

W.A. Cribbs[147a,147b], M. Crispin Ortuzar[121], M. Cristinziani[23], V. Croft[107], G. Crosetti[39a,39b], T. Cuhadar Donszelmann[140], J. Cummings[176], M. Curatolo[49], J. Cúth[85], C. Cuthbert[151], H. Czirr[142], P. Czodrowski[3], S. D'Auria[55], M. D'Onofrio[76], M.J. Da Cunha Sargedas De Sousa[127a,127b], C. Da Via[86], W. Dabrowski[40a], T. Dai[91], O. Dale[15], F. Dallaire[96], C. Dallapiccola[88], M. Dam[38], J.R. Dandoy[33], N.P. Dang[50], A.C. Daniells[19], N.S. Dann[86], M. Danninger[168], M. Dano Hoffmann[137], V. Dao[50], G. Darbo[52a], S. Darmora[8], J. Dassoulas[3], A. Dattagupta[63], W. Davey[23], C. David[169], T. Davidek[130], M. Davies[154], P. Davison[80], Y. Davygora[60a], E. Dawe[90], I. Dawson[140], R.K. Daya-Ishmukhametova[88], K. De[8], R. de Asmundis[105a], A. De Benedetti[114], S. De Castro[22a,22b], S. De Cecco[82], N. De Groot[107], P. de Jong[108], H. De la Torre[84], F. De Lorenzi[66], D. De Pedis[133a], A. De Salvo[133a], U. De Sanctis[150], A. De Santo[150], J.B. De Vivie De Regie[118], W.J. Dearnaley[74], R. Debbe[27], C. Debenedetti[138], D.V. Dedovich[67], I. Deigaard[108], J. Del Peso[84], T. Del Prete[125a,125b], D. Delgove[118], F. Deliot[137], C.M. Delitzsch[51], M. Deliyergiyev[77], A. Dell'Acqua[32], L. Dell'Asta[24], M. Dell'Orso[125a,125b], M. Della Pietra[105a,k], D. della Volpe[51], M. Delmastro[5], P.A. Delsart[57], C. Deluca[108], D.A. DeMarco[159], S. Demers[176], M. Demichev[67], A. Demilly[82], S.P. Denisov[131], D. Denysiuk[137], D. Derendarz[41], J.E. Derkaoui[136d], F. Derue[82], P. Dervan[76], K. Desch[23], C. Deterre[44], K. Dette[45], P.O. Deviveiros[32], A. Dewhurst[132], S. Dhaliwal[25], A. Di Ciaccio[134a,134b], L. Di Ciaccio[5], W.K. Di Clemente[123], C. Di Donato[133a,133b], A. Di Girolamo[32], B. Di Girolamo[32], B. Di Micco[135a,135b], R. Di Nardo[49], A. Di Simone[50], R. Di Sipio[159], D. Di Valentino[31], C. Diaconu[87], M. Diamond[159], F.A. Dias[48], M.A. Diaz[34a], E.B. Diehl[91], J. Dietrich[17], S. Diglio[87], A. Dimitrievska[14], J. Dingfelder[23], P. Dita[28b], S. Dita[28b], F. Dittus[32], F. Djama[87], T. Djobava[53b], J.I. Djuvsland[60a], M.A.B. do Vale[26c], D. Dobos[32], M. Dobre[28b], C. Doglioni[83], T. Dohmae[156], J. Dolejsi[130], Z. Dolezal[130], B.A. Dolgoshein[99,*], M. Donadelli[26d], S. Donati[125a,125b], P. Dondero[122a,122b], J. Donini[36], J. Dopke[132], A. Doria[105a], M.T. Dova[73], A.T. Doyle[55], E. Drechsler[56], M. Dris[10], Y. Du[35d], J. Duarte-Campderros[154], E. Duchovni[172], G. Duckeck[101], O.A. Ducu[28b], D. Duda[108], A. Dudarev[32], L. Duflot[118], L. Duguid[79], M. Dührssen[32], M. Dunford[60a], H. Duran Yildiz[4a], M. Düren[54], A. Durglishvili[53b], D. Duschinger[46], B. Dutta[44], M. Dyndal[40a], C. Eckardt[44], K.M. Ecker[102], R.C. Edgar[91], W. Edson[2], N.C. Edwards[48], T. Eifert[32], G. Eigen[15], K. Einsweiler[16], T. Ekelof[165], M. El Kacimi[136c], V. Ellajosyula[87], M. Ellert[165], S. Elles[5], F. Ellinghaus[175], A.A. Elliot[169], N. Ellis[32], J. Elmsheuser[27], M. Elsing[32], D. Emeliyanov[132], Y. Enari[156], O.C. Endner[85], M. Endo[119], J.S. Ennis[170], J. Erdmann[45], A. Ereditato[18], G. Ernis[175], J. Ernst[2], M. Ernst[27], S. Errede[166], E. Ertel[85], M. Escalier[118], H. Esch[45], C. Escobar[126], B. Esposito[49], A.I. Etienvre[137], E. Etzion[154], H. Evans[63], A. Ezhilov[124], F. Fabbri[22a,22b], L. Fabbri[22a,22b], G. Facini[33], R.M. Fakhrutdinov[131], S. Falciano[133a], R.J. Falla[80], J. Faltova[130], Y. Fang[35a], M. Fanti[93a,93b], A. Farbin[8], A. Farilla[135a], C. Farina[126], T. Farooque[13], S. Farrell[16], S.M. Farrington[170], P. Farthouat[32], F. Fassi[136e], P. Fassnacht[32], D. Fassouliotis[9], M. Faucci Giannelli[79], A. Favareto[52a,52b], W.J. Fawcett[121], L. Fayard[118], O.L. Fedin[124,m], W. Fedorko[168], S. Feigl[120], L. Feligioni[87], C. Feng[35d], E.J. Feng[32], H. Feng[91], A.B. Fenyuk[131], L. Feremenga[8], P. Fernandez Martinez[167], S. Fernandez Perez[13], J. Ferrando[55], A. Ferrari[165], P. Ferrari[108], R. Ferrari[122a], D.E. Ferreira de Lima[55], A. Ferrer[167], D. Ferrere[51], C. Ferretti[91], A. Ferretto Parodi[52a,52b], F. Fiedler[85], A. Filipčič[77], M. Filipuzzi[44], F. Filthaut[107], M. Fincke-Keeler[169], K.D. Finelli[151], M.C.N. Fiolhais[127a,127c], L. Fiorini[167], A. Firan[42], A. Fischer[2], C. Fischer[13], J. Fischer[175], W.C. Fisher[92], N. Flaschel[44], I. Fleck[142], P. Fleischmann[91], G.T. Fletcher[140], G. Fletcher[78], R.R.M. Fletcher[123], T. Flick[175], A. Floderus[83], L.R. Flores Castillo[62a], M.J. Flowerdew[102], G.T. Forcolin[86], A. Formica[137], A. Forti[86], A.G. Foster[19], D. Fournier[118], H. Fox[74], S. Fracchia[13], P. Francavilla[82], M. Franchini[22a,22b], D. Francis[32], L. Franconi[120], M. Franklin[59], M. Frate[163], M. Fraternali[122a,122b], D. Freeborn[80], S.M. Fressard-Batraneanu[32], F. Friedrich[46], D. Froidevaux[32], J.A. Frost[121], C. Fukunaga[157], E. Fullana Torregrosa[85], T. Fusayasu[103], J. Fuster[167], C. Gabaldon[57], O. Gabizon[175], A. Gabrielli[22a,22b], A. Gabrielli[16], G.P. Gach[40a], S. Gadatsch[32], S. Gadomski[51], G. Gagliardi[52a,52b], L.G. Gagnon[96], P. Gagnon[63], C. Galea[107], B. Galhardo[127a,127c],

E.J. Gallas[121], B.J. Gallop[132], P. Gallus[129], G. Galster[38], K.K. Gan[112], J. Gao[35b,87], Y. Gao[48], Y.S. Gao[144,f], F.M. Garay Walls[48], C. García[167], J.E. García Navarro[167], M. Garcia-Sciveres[16], R.W. Gardner[33], N. Garelli[144], V. Garonne[120], A. Gascon Bravo[44], C. Gatti[49], A. Gaudiello[52a,52b], G. Gaudio[122a], B. Gaur[142], L. Gauthier[96], I.L. Gavrilenko[97], C. Gay[168], G. Gaycken[23], E.N. Gazis[10], Z. Gecse[168], C.N.P. Gee[132], Ch. Geich-Gimbel[23], M.P. Geisler[60a], C. Gemme[52a], M.H. Genest[57], C. Geng[35b,n], S. Gentile[133a,133b], S. George[79], D. Gerbaudo[163], A. Gershon[154], S. Ghasemi[142], H. Ghazlane[136b], M. Ghneimat[23], B. Giacobbe[22a], S. Giagu[133a,133b], P. Giannetti[125a,125b], B. Gibbard[27], S.M. Gibson[79], M. Gignac[168], M. Gilchriese[16], T.P.S. Gillam[30], D. Gillberg[31], G. Gilles[175], D.M. Gingrich[3,d], N. Giokaris[9], M.P. Giordani[164a,164c], F.M. Giorgi[22a], F.M. Giorgi[17], P.F. Giraud[137], P. Giromini[59], D. Giugni[93a], F. Giuli[121], C. Giuliani[102], M. Giulini[60b], B.K. Gjelsten[120], S. Gkaitatzis[155], I. Gkialas[155], E.L. Gkougkousis[118], L.K. Gladilin[100], C. Glasman[84], J. Glatzer[32], P.C.F. Glaysher[48], A. Glazov[44], M. Goblirsch-Kolb[102], J. Godlewski[41], S. Goldfarb[91], T. Golling[51], D. Golubkov[131], A. Gomes[127a,127b,127d], R. Gonçalo[127a], J. Goncalves Pinto Firmino Da Costa[137], L. Gonella[19], A. Gongadze[67], S. González de la Hoz[167], G. Gonzalez Parra[13], S. Gonzalez-Sevilla[51], L. Goossens[32], P.A. Gorbounov[98], H.A. Gordon[27], I. Gorelov[106], B. Gorini[32], E. Gorini[75a,75b], A. Gorišek[77], E. Gornicki[41], A.T. Goshaw[47], C. Gössling[45], M.I. Gostkin[67], C.R. Goudet[118], D. Goujdami[136c], A.G. Goussiou[139], N. Govender[146b,o], E. Gozani[153], L. Graber[56], I. Grabowska-Bold[40a], P.O.J. Gradin[57], P. Grafström[22a,22b], J. Gramling[51], E. Gramstad[120], S. Grancagnolo[17], V. Gratchev[124], H.M. Gray[32], E. Graziani[135a], Z.D. Greenwood[81,p], C. Grefe[23], K. Gregersen[80], I.M. Gregor[44], P. Grenier[144], K. Grevtsov[5], J. Griffiths[8], A.A. Grillo[138], K. Grimm[74], S. Grinstein[13,q], Ph. Gris[36], J.-F. Grivaz[118], S. Groh[85], J.P. Grohs[46], E. Gross[172], J. Grosse-Knetter[56], G.C. Grossi[81], Z.J. Grout[150], L. Guan[91], W. Guan[173], J. Guenther[129], F. Guescini[51], D. Guest[163], O. Gueta[154], E. Guido[52a,52b], T. Guillemin[5], S. Guindon[2], U. Gul[55], C. Gumpert[32], J. Guo[35e], Y. Guo[35b,n], S. Gupta[121], G. Gustavino[133a,133b], P. Gutierrez[114], N.G. Gutierrez Ortiz[80], C. Gutschow[46], C. Guyot[137], C. Gwenlan[121], C.B. Gwilliam[76], A. Haas[111], C. Haber[16], H.K. Hadavand[8], N. Haddad[136e], A. Hadef[87], P. Haefner[23], S. Hageböck[23], Z. Hajduk[41], H. Hakobyan[177,*], M. Haleem[44], J. Haley[115], D. Hall[121], G. Halladjian[92], G.D. Hallewell[87], K. Hamacher[175], P. Hamal[116], K. Hamano[169], A. Hamilton[146a], G.N. Hamity[140], P.G. Hamnett[44], L. Han[35b], K. Hanagaki[68,r], K. Hanawa[156], M. Hance[138], B. Haney[123], P. Hanke[60a], R. Hanna[137], J.B. Hansen[38], J.D. Hansen[38], M.C. Hansen[23], P.H. Hansen[38], K. Hara[161], A.S. Hard[173], T. Harenberg[175], F. Hariri[118], S. Harkusha[94], R.D. Harrington[48], P.F. Harrison[170], F. Hartjes[108], M. Hasegawa[69], Y. Hasegawa[141], A. Hasib[114], S. Hassani[137], S. Haug[18], R. Hauser[92], L. Hauswald[46], M. Havranek[128], C.M. Hawkes[19], R.J. Hawkings[32], A.D. Hawkins[83], D. Hayden[92], C.P. Hays[121], J.M. Hays[78], H.S. Hayward[76], S.J. Haywood[132], S.J. Head[19], T. Heck[85], V. Hedberg[83], L. Heelan[8], S. Heim[123], T. Heim[16], B. Heinemann[16], J.J. Heinrich[101], L. Heinrich[111], C. Heinz[54], J. Hejbal[128], L. Helary[24], S. Hellman[147a,147b], C. Helsens[32], J. Henderson[121], R.C.W. Henderson[74], Y. Heng[173], S. Henkelmann[168], A.M. Henriques Correia[32], S. Henrot-Versille[118], G.H. Herbert[17], Y. Hernández Jiménez[167], G. Herten[50], R. Hertenberger[101], L. Hervas[32], G.G. Hesketh[80], N.P. Hessey[108], J.W. Hetherly[42], R. Hickling[78], E. Higón-Rodriguez[167], E. Hill[169], J.C. Hill[30], K.H. Hiller[44], S.J. Hillier[19], I. Hinchliffe[16], E. Hines[123], R.R. Hinman[16], M. Hirose[158], D. Hirschbuehl[175], J. Hobbs[149], N. Hod[108], M.C. Hodgkinson[140], P. Hodgson[140], A. Hoecker[32], M.R. Hoeferkamp[106], F. Hoenig[101], M. Hohlfeld[85], D. Hohn[23], T.R. Holmes[16], M. Homann[45], T.M. Hong[126], B.H. Hooberman[166], W.H. Hopkins[117], Y. Horii[104], A.J. Horton[143], J-Y. Hostachy[57], S. Hou[152], A. Hoummada[136a], J. Howard[121], J. Howarth[44], M. Hrabovsky[116], I. Hristova[17], J. Hrivnac[118], T. Hryn'ova[5], A. Hrynevich[95], C. Hsu[146c], P.J. Hsu[152,s], S.-C. Hsu[139], D. Hu[37], Q. Hu[35b], Y. Huang[44], Z. Hubacek[129], F. Hubaut[87], F. Huegging[23], T.B. Huffman[121], E.W. Hughes[37], G. Hughes[74], M. Huhtinen[32], T.A. Hülsing[85], N. Huseynov[67,b], J. Huston[92], J. Huth[59], G. Iacobucci[51], G. Iakovidis[27], I. Ibragimov[142], L. Iconomidou-Fayard[118], E. Ideal[176], Z. Idrissi[136e], P. Iengo[32], O. Igonkina[108,t],

T. Iizawa[171], Y. Ikegami[68], M. Ikeno[68], Y. Ilchenko[11,u], D. Iliadis[155], N. Ilic[144], T. Ince[102], G. Introzzi[122a,122b], P. Ioannou[9,*], M. Iodice[135a], K. Iordanidou[37], V. Ippolito[59], A. Irles Quiles[167], C. Isaksson[165], M. Ishino[70], M. Ishitsuka[158], R. Ishmukhametov[112], C. Issever[121], S. Istin[20a], F. Ito[161], J.M. Iturbe Ponce[86], R. Iuppa[134a,134b], J. Ivarsson[83], W. Iwanski[41], H. Iwasaki[68], J.M. Izen[43], V. Izzo[105a], S. Jabbar[3], B. Jackson[123], M. Jackson[76], P. Jackson[1], V. Jain[2], K.B. Jakobi[85], K. Jakobs[50], S. Jakobsen[32], T. Jakoubek[128], D.O. Jamin[115], D.K. Jana[81], E. Jansen[80], R. Jansky[64], J. Janssen[23], M. Janus[56], G. Jarlskog[83], N. Javadov[67,b], T. Javůrek[50], F. Jeanneau[137], L. Jeanty[16], J. Jejelava[53a,v], G.-Y. Jeng[151], D. Jennens[90], P. Jenni[50,w], J. Jentzsch[45], C. Jeske[170], S. Jézéquel[5], H. Ji[173], J. Jia[149], H. Jiang[66], Y. Jiang[35b], S. Jiggins[80], J. Jimenez Pena[167], S. Jin[35a], A. Jinaru[28b], O. Jinnouchi[158], P. Johansson[140], K.A. Johns[7], W.J. Johnson[139], K. Jon-And[147a,147b], G. Jones[170], R.W.L. Jones[74], S. Jones[7], T.J. Jones[76], J. Jongmanns[60a], P.M. Jorge[127a,127b], J. Jovicevic[160a], X. Ju[173], A. Juste Rozas[13,q], M.K. Köhler[172], A. Kaczmarska[41], M. Kado[118], H. Kagan[112], M. Kagan[144], S.J. Kahn[87], E. Kajomovitz[47], C.W. Kalderon[121], A. Kaluza[85], S. Kama[42], A. Kamenshchikov[131], N. Kanaya[156], S. Kaneti[30], L. Kanjir[77], V.A. Kantserov[99], J. Kanzaki[68], B. Kaplan[111], L.S. Kaplan[173], A. Kapliy[33], D. Kar[146c], K. Karakostas[10], A. Karamaoun[3], N. Karastathis[10], M.J. Kareem[56], E. Karentzos[10], M. Karnevskiy[85], S.N. Karpov[67], Z.M. Karpova[67], K. Karthik[111], V. Kartvelishvili[74], A.N. Karyukhin[131], K. Kasahara[161], L. Kashif[173], R.D. Kass[112], A. Kastanas[15], Y. Kataoka[156], C. Kato[156], A. Katre[51], J. Katzy[44], K. Kawagoe[72], T. Kawamoto[156], G. Kawamura[56], S. Kazama[156], V.F. Kazanin[110,c], R. Keeler[169], R. Kehoe[42], J.S. Keller[44], J.J. Kempster[79], K Kentaro[104], H. Keoshkerian[86], O. Kepka[128], B.P. Kerševan[77], S. Kersten[175], R.A. Keyes[89], F. Khalil-zada[12], H. Khandanyan[147a,147b], A. Khanov[115], A.G. Kharlamov[110,c], T.J. Khoo[30], V. Khovanskiy[98], E. Khramov[67], J. Khubua[53b,x], S. Kido[69], H.Y. Kim[8], S.H. Kim[161], Y.K. Kim[33], N. Kimura[155], O.M. Kind[17], B.T. King[76], M. King[167], S.B. King[168], J. Kirk[132], A.E. Kiryunin[102], T. Kishimoto[69], D. Kisielewska[40a], F. Kiss[50], K. Kiuchi[161], O. Kivernyk[137], E. Kladiva[145b], M.H. Klein[37], M. Klein[76], U. Klein[76], K. Kleinknecht[85], P. Klimek[147a,147b], A. Klimentov[27], R. Klingenberg[45], J.A. Klinger[140], T. Klioutchnikova[32], E.-E. Kluge[60a], P. Kluit[108], S. Kluth[102], J. Knapik[41], E. Kneringer[64], E.B.F.G. Knoops[87], A. Knue[55], A. Kobayashi[156], D. Kobayashi[158], T. Kobayashi[156], M. Kobel[46], M. Kocian[144], P. Kodys[130], T. Koffas[31], E. Koffeman[108], L.A. Kogan[121], T. Koi[144], H. Kolanoski[17], M. Kolb[60b], I. Koletsou[5], A.A. Komar[97,*], Y. Komori[156], T. Kondo[68], N. Kondrashova[44], K. Köneke[50], A.C. König[107], T. Kono[68,y], R. Konoplich[111,z], N. Konstantinidis[80], R. Kopeliansky[63], S. Koperny[40a], L. Köpke[85], A.K. Kopp[50], K. Korcyl[41], K. Kordas[155], A. Korn[80], A.A. Korol[110,c], I. Korolkov[13], E.V. Korolkova[140], O. Kortner[102], S. Kortner[102], T. Kosek[130], V.V. Kostyukhin[23], A. Kotwal[47], A. Kourkoumeli-Charalampidi[155], C. Kourkoumelis[9], V. Kouskoura[27], A. Koutsman[160a], A.B. Kowalewska[41], R. Kowalewski[169], T.Z. Kowalski[40a], W. Kozanecki[137], A.S. Kozhin[131], V.A. Kramarenko[100], G. Kramberger[77], D. Krasnopevtsev[99], M.W. Krasny[82], A. Krasznahorkay[32], J.K. Kraus[23], A. Kravchenko[27], M. Kretz[60c], J. Kretzschmar[76], K. Kreutzfeldt[54], P. Krieger[159], K. Krizka[33], K. Kroeninger[45], H. Kroha[102], J. Kroll[123], J. Kroseberg[23], J. Krstic[14], U. Kruchonak[67], H. Krüger[23], N. Krumnack[66], A. Kruse[173], M.C. Kruse[47], M. Kruskal[24], T. Kubota[90], H. Kucuk[80], S. Kuday[4b], J.T. Kuechler[175], S. Kuehn[50], A. Kugel[60c], F. Kuger[174], A. Kuhl[138], T. Kuhl[44], V. Kukhtin[67], R. Kukla[137], Y. Kulchitsky[94], S. Kuleshov[34b], M. Kuna[133a,133b], T. Kunigo[70], A. Kupco[128], H. Kurashige[69], Y.A. Kurochkin[94], V. Kus[128], E.S. Kuwertz[169], M. Kuze[158], J. Kvita[116], T. Kwan[169], D. Kyriazopoulos[140], A. La Rosa[102], J.L. La Rosa Navarro[26d], L. La Rotonda[39a,39b], C. Lacasta[167], F. Lacava[133a,133b], J. Lacey[31], H. Lacker[17], D. Lacour[82], V.R. Lacuesta[167], E. Ladygin[67], R. Lafaye[5], B. Laforge[82], T. Lagouri[176], S. Lai[56], S. Lammers[63], W. Lampl[7], E. Lançon[137], U. Landgraf[50], M.P.J. Landon[78], V.S. Lang[60a], J.C. Lange[13], A.J. Lankford[163], F. Lanni[27], K. Lantzsch[23], A. Lanza[122a], S. Laplace[82], C. Lapoire[32], J.F. Laporte[137], T. Lari[93a], F. Lasagni Manghi[22a,22b], M. Lassnig[32], P. Laurelli[49], W. Lavrijsen[16], A.T. Law[138], P. Laycock[76], T. Lazovich[59], M. Lazzaroni[93a,93b], O. Le Dortz[82], E. Le Guirriec[87], E. Le Menedeu[13],

E.P. Le Quilleuc[137], M. LeBlanc[169], T. LeCompte[6], F. Ledroit-Guillon[57], C.A. Lee[27], S.C. Lee[152], L. Lee[1], G. Lefebvre[82], M. Lefebvre[169], F. Legger[101], C. Leggett[16], A. Lehan[76], G. Lehmann Miotto[32], X. Lei[7], W.A. Leight[31], A. Leisos[155,aa], A.G. Leister[176], M.A.L. Leite[26d], R. Leitner[130], D. Lellouch[172], B. Lemmer[56], K.J.C. Leney[80], T. Lenz[23], B. Lenzi[32], R. Leone[7], S. Leone[125a,125b], C. Leonidopoulos[48], S. Leontsinis[10], G. Lerner[150], C. Leroy[96], A.A.J. Lesage[137], C.G. Lester[30], M. Levchenko[124], J. Levêque[5], D. Levin[91], L.J. Levinson[172], M. Levy[19], A.M. Leyko[23], M. Leyton[43], B. Li[35b,n], H. Li[149], H.L. Li[33], L. Li[47], L. Li[35e], Q. Li[35a], S. Li[47], X. Li[86], Y. Li[142], Z. Liang[138], H. Liao[36], B. Liberti[134a], A. Liblong[159], P. Lichard[32], K. Lie[166], J. Liebal[23], W. Liebig[15], C. Limbach[23], A. Limosani[151], S.C. Lin[152,ab], T.H. Lin[85], B.E. Lindquist[149], E. Lipeles[123], A. Lipniacka[15], M. Lisovyi[60b], T.M. Liss[166], D. Lissauer[27], A. Lister[168], A.M. Litke[138], B. Liu[152,ac], D. Liu[152], H. Liu[91], H. Liu[27], J. Liu[87], J.B. Liu[35b], K. Liu[87], L. Liu[166], M. Liu[47], M. Liu[35b], Y.L. Liu[35b], Y. Liu[35b], M. Livan[122a,122b], A. Lleres[57], J. Llorente Merino[84], S.L. Lloyd[78], F. Lo Sterzo[152], E. Lobodzinska[44], P. Loch[7], W.S. Lockman[138], F.K. Loebinger[86], A.E. Loevschall-Jensen[38], K.M. Loew[25], A. Loginov[176], T. Lohse[17], K. Lohwasser[44], M. Lokajicek[128], B.A. Long[24], J.D. Long[166], R.E. Long[74], L. Longo[75a,75b], K.A. Looper[112], L. Lopes[127a], D. Lopez Mateos[59], B. Lopez Paredes[140], I. Lopez Paz[13], A. Lopez Solis[82], J. Lorenz[101], N. Lorenzo Martinez[63], M. Losada[21], P.J. Lösel[101], X. Lou[35a], A. Lounis[118], J. Love[6], P.A. Love[74], H. Lu[62a], N. Lu[91], H.J. Lubatti[139], C. Luci[133a,133b], A. Lucotte[57], C. Luedtke[50], F. Luehring[63], W. Lukas[64], L. Luminari[133a], O. Lundberg[147a,147b], B. Lund-Jensen[148], D. Lynn[27], R. Lysak[128], E. Lytken[83], V. Lyubushkin[67], H. Ma[27], L.L. Ma[35d], Y. Ma[35d], G. Maccarrone[49], A. Macchiolo[102], C.M. Macdonald[140], B. Maček[77], J. Machado Miguens[123,127b], D. Madaffari[87], R. Madar[36], H.J. Maddocks[165], W.F. Mader[46], A. Madsen[44], J. Maeda[69], S. Maeland[15], T. Maeno[27], A. Maevskiy[100], E. Magradze[56], J. Mahlstedt[108], C. Maiani[118], C. Maidantchik[26a], A.A. Maier[102], T. Maier[101], A. Maio[127a,127b,127d], S. Majewski[117], Y. Makida[68], N. Makovec[118], B. Malaescu[82], Pa. Malecki[41], V.P. Maleev[124], F. Malek[57], U. Mallik[65], D. Malon[6], C. Malone[144], S. Maltezos[10], S. Malyukov[32], J. Mamuzic[167], G. Mancini[49], B. Mandelli[32], L. Mandelli[93a], I. Mandić[77], J. Maneira[127a,127b], L. Manhaes de Andrade Filho[26b], J. Manjarres Ramos[160b], A. Mann[101], B. Mansoulie[137], R. Mantifel[89], M. Mantoani[56], S. Manzoni[93a,93b], L. Mapelli[32], G. Marceca[29], L. March[51], G. Marchiori[82], M. Marcisovsky[128], M. Marjanovic[14], D.E. Marley[91], F. Marroquim[26a], S.P. Marsden[86], Z. Marshall[16], L.F. Marti[18], S. Marti-Garcia[167], B. Martin[92], T.A. Martin[170], V.J. Martin[48], B. Martin dit Latour[15], M. Martinez[13,q], S. Martin-Haugh[132], V.S. Martoiu[28b], A.C. Martyniuk[80], M. Marx[139], F. Marzano[133a], A. Marzin[32], L. Masetti[85], T. Mashimo[156], R. Mashinistov[97], J. Masik[86], A.L. Maslennikov[110,c], I. Massa[22a,22b], L. Massa[22a,22b], P. Mastrandrea[5], A. Mastroberardino[39a,39b], T. Masubuchi[156], P. Mättig[175], J. Mattmann[85], J. Maurer[28b], S.J. Maxfield[76], D.A. Maximov[110,c], R. Mazini[152], S.M. Mazza[93a,93b], N.C. Mc Fadden[106], G. Mc Goldrick[159], S.P. Mc Kee[91], A. McCarn[91], R.L. McCarthy[149], T.G. McCarthy[31], L.I. McClymont[80], K.W. McFarlane[58,*], J.A. Mcfayden[80], G. Mchedlidze[56], S.J. McMahon[132], R.A. McPherson[169,l], M. Medinnis[44], S. Meehan[139], S. Mehlhase[101], A. Mehta[76], K. Meier[60a], C. Meineck[101], B. Meirose[43], B.R. Mellado Garcia[146c], F. Meloni[18], A. Mengarelli[22a,22b], S. Menke[102], E. Meoni[162], K.M. Mercurio[59], S. Mergelmeyer[17], P. Mermod[51], L. Merola[105a,105b], C. Meroni[93a], F.S. Merritt[33], A. Messina[133a,133b], J. Metcalfe[6], A.S. Mete[163], C. Meyer[85], C. Meyer[123], J-P. Meyer[137], J. Meyer[108], H. Meyer Zu Theenhausen[60a], R.P. Middleton[132], S. Miglioranzi[164a,164c], L. Mijović[23], G. Mikenberg[172], M. Mikestikova[128], M. Mikuž[77], M. Milesi[90], A. Milic[32], D.W. Miller[33], C. Mills[48], A. Milov[172], D.A. Milstead[147a,147b], A.A. Minaenko[131], Y. Minami[156], I.A. Minashvili[67], A.I. Mincer[111], B. Mindur[40a], M. Mineev[67], Y. Ming[173], L.M. Mir[13], K.P. Mistry[123], T. Mitani[171], J. Mitrevski[101], V.A. Mitsou[167], A. Miucci[51], P.S. Miyagawa[140], J.U. Mjörnmark[83], T. Moa[147a,147b], K. Mochizuki[87], S. Mohapatra[37], W. Mohr[50], S. Molander[147a,147b], R. Moles-Valls[23], R. Monden[70], M.C. Mondragon[92], K. Mönig[44], J. Monk[38], E. Monnier[87], A. Montalbano[149], J. Montejo Berlingen[32], F. Monticelli[73],

S. Monzani[93a,93b], R.W. Moore[3], N. Morange[118], D. Moreno[21], M. Moreno Llácer[56], P. Morettini[52a], D. Mori[143], T. Mori[156], M. Morii[59], M. Morinaga[156], V. Morisbak[120], S. Moritz[85], A.K. Morley[151], G. Mornacchi[32], J.D. Morris[78], S.S. Mortensen[38], L. Morvaj[149], M. Mosidze[53b], J. Moss[144], K. Motohashi[158], R. Mount[144], E. Mountricha[27], S.V. Mouraviev[97,*], E.J.W. Moyse[88], S. Muanza[87], R.D. Mudd[19], F. Mueller[102], J. Mueller[126], R.S.P. Mueller[101], T. Mueller[30], D. Muenstermann[74], P. Mullen[55], G.A. Mullier[18], F.J. Munoz Sanchez[86], J.A. Murillo Quijada[19], W.J. Murray[170,132], H. Musheghyan[56], M. Muškinja[77], A.G. Myagkov[131,*ad*], M. Myska[129], B.P. Nachman[144], O. Nackenhorst[51], J. Nadal[56], K. Nagai[121], R. Nagai[68,*y*], K. Nagano[68], Y. Nagasaka[61], K. Nagata[161], M. Nagel[102], E. Nagy[87], A.M. Nairz[32], Y. Nakahama[32], K. Nakamura[68], T. Nakamura[156], I. Nakano[113], H. Namasivayam[43], R.F. Naranjo Garcia[44], R. Narayan[11], D.I. Narrias Villar[60a], I. Naryshkin[124], T. Naumann[44], G. Navarro[21], R. Nayyar[7], H.A. Neal[91], P.Yu. Nechaeva[97], T.J. Neep[86], P.D. Nef[144], A. Negri[122a,122b], M. Negrini[22a], S. Nektarijevic[107], C. Nellist[118], A. Nelson[163], S. Nemecek[128], P. Nemethy[111], A.A. Nepomuceno[26a], M. Nessi[32,*ae*], M.S. Neubauer[166], M. Neumann[175], R.M. Neves[111], P. Nevski[27], P.R. Newman[19], D.H. Nguyen[6], R.B. Nickerson[121], R. Nicolaidou[137], B. Nicquevert[32], J. Nielsen[138], A. Nikiforov[17], V. Nikolaenko[131,*ad*], I. Nikolic-Audit[82], K. Nikolopoulos[19], J.K. Nilsen[120], P. Nilsson[27], Y. Ninomiya[156], A. Nisati[133a], R. Nisius[102], T. Nobe[156], L. Nodulman[6], M. Nomachi[119], I. Nomidis[31], T. Nooney[78], S. Norberg[114], M. Nordberg[32], N. Norjoharuddeen[121], O. Novgorodova[46], S. Nowak[102], M. Nozaki[68], L. Nozka[116], K. Ntekas[10], E. Nurse[80], F. Nuti[90], F. O'grady[7], D.C. O'Neil[143], A.A. O'Rourke[44], V. O'Shea[55], F.G. Oakham[31,*d*], H. Oberlack[102], T. Obermann[23], J. Ocariz[82], A. Ochi[69], I. Ochoa[37], J.P. Ochoa-Ricoux[34a], S. Oda[72], S. Odaka[68], H. Ogren[63], A. Oh[86], S.H. Oh[47], C.C. Ohm[16], H. Ohman[165], H. Oide[32], H. Okawa[161], Y. Okumura[33], T. Okuyama[68], A. Olariu[28b], L.F. Oleiro Seabra[127a], S.A. Olivares Pino[48], D. Oliveira Damazio[27], A. Olszewski[41], J. Olszowska[41], A. Onofre[127a,127e], K. Onogi[104], P.U.E. Onyisi[11,*u*], C.J. Oram[160a], M.J. Oreglia[33], Y. Oren[154], D. Orestano[135a,135b], N. Orlando[62b], R.S. Orr[159], B. Osculati[52a,52b], R. Ospanov[86], G. Otero y Garzon[29], H. Otono[72], M. Ouchrif[136d], F. Ould-Saada[120], A. Ouraou[137], K.P. Oussoren[108], Q. Ouyang[35a], M. Owen[55], R.E. Owen[19], V.E. Ozcan[20a], N. Ozturk[8], K. Pachal[143], A. Pacheco Pages[13], C. Padilla Aranda[13], M. Pagáčová[50], S. Pagan Griso[16], F. Paige[27], P. Pais[88], K. Pajchel[120], G. Palacino[160b], S. Palestini[32], M. Palka[40b], D. Pallin[36], A. Palma[127a,127b], E.St. Panagiotopoulou[10], C.E. Pandini[82], J.G. Panduro Vazquez[79], P. Pani[147a,147b], S. Panitkin[27], D. Pantea[28b], L. Paolozzi[51], Th.D. Papadopoulou[10], K. Papageorgiou[155], A. Paramonov[6], D. Paredes Hernandez[176], A.J. Parker[74], M.A. Parker[30], K.A. Parker[140], F. Parodi[52a,52b], J.A. Parsons[37], U. Parzefall[50], V.R. Pascuzzi[159], E. Pasqualucci[133a], S. Passaggio[52a], F. Pastore[135a,135b,*], Fr. Pastore[79], G. Pásztor[31,*af*], S. Pataraia[175], N.D. Patel[151], J.R. Pater[86], T. Pauly[32], J. Pearce[169], B. Pearson[114], L.E. Pedersen[38], M. Pedersen[120], S. Pedraza Lopez[167], R. Pedro[127a,127b], S.V. Peleganchuk[110,*c*], D. Pelikan[165], O. Penc[128], C. Peng[35a], H. Peng[35b], J. Penwell[63], B.S. Peralva[26b], M.M. Perego[137], D.V. Perepelitsa[27], E. Perez Codina[160a], L. Perini[93a,93b], H. Pernegger[32], S. Perrella[105a,105b], R. Peschke[44], V.D. Peshekhonov[67], K. Peters[44], R.F.Y. Peters[86], B.A. Petersen[32], T.C. Petersen[38], E. Petit[57], A. Petridis[1], C. Petridou[155], P. Petroff[118], E. Petrolo[133a], M. Petrov[121], F. Petrucci[135a,135b], N.E. Pettersson[158], A. Peyaud[137], R. Pezoa[34b], P.W. Phillips[132], G. Piacquadio[144], E. Pianori[170], A. Picazio[88], E. Piccaro[78], M. Piccinini[22a,22b], M.A. Pickering[121], R. Piegaia[29], J.E. Pilcher[33], A.D. Pilkington[86], A.W.J. Pin[86], J. Pina[127a,127b,127d], M. Pinamonti[164a,164c,*ag*], J.L. Pinfold[3], A. Pingel[38], S. Pires[82], H. Pirumov[44], M. Pitt[172], L. Plazak[145a], M.-A. Pleier[27], V. Pleskot[85], E. Plotnikova[67], P. Plucinski[147a,147b], D. Pluth[66], R. Poettgen[147a,147b], L. Poggioli[118], D. Pohl[23], G. Polesello[122a], A. Poley[44], A. Policicchio[39a,39b], R. Polifka[159], A. Polini[22a], C.S. Pollard[55], V. Polychronakos[27], K. Pommès[32], L. Pontecorvo[133a], B.G. Pope[92], G.A. Popeneciu[28c], D.S. Popovic[14], A. Poppleton[32], S. Pospisil[129], K. Potamianos[16], I.N. Potrap[67], C.J. Potter[30], C.T. Potter[117], G. Poulard[32], J. Poveda[32], V. Pozdnyakov[67], M.E. Pozo Astigarraga[32], P. Pralavorio[87], A. Pranko[16], S. Prell[66], D. Price[86], L.E. Price[6], M. Primavera[75a], S. Prince[89], M. Proissl[48],

K. Prokofiev[62c], F. Prokoshin[34b], S. Protopopescu[27], J. Proudfoot[6], M. Przybycien[40a], D. Puddu[135a,135b], D. Puldon[149], M. Purohit[27,ah], P. Puzo[118], J. Qian[91], G. Qin[55], Y. Qin[86], A. Quadt[56], W.B. Quayle[164a,164b], M. Queitsch-Maitland[86], D. Quilty[55], S. Raddum[120], V. Radeka[27], V. Radescu[60b], S.K. Radhakrishnan[149], P. Radloff[117], P. Rados[90], F. Ragusa[93a,93b], G. Rahal[178], J.A. Raine[86], S. Rajagopalan[27], M. Rammensee[32], C. Rangel-Smith[165], M.G. Ratti[93a,93b], F. Rauscher[101], S. Rave[85], T. Ravenscroft[55], M. Raymond[32], A.L. Read[120], N.P. Readioff[76], D.M. Rebuzzi[122a,122b], A. Redelbach[174], G. Redlinger[27], R. Reece[138], K. Reeves[43], L. Rehnisch[17], J. Reichert[123], H. Reisin[29], C. Rembser[32], H. Ren[35a], M. Rescigno[133a], S. Resconi[93a], O.L. Rezanova[110,c], P. Reznicek[130], R. Rezvani[96], R. Richter[102], S. Richter[80], E. Richter-Was[40b], O. Ricken[23], M. Ridel[82], P. Rieck[17], C.J. Riegel[175], J. Rieger[56], O. Rifki[114], M. Rijssenbeek[149], A. Rimoldi[122a,122b], L. Rinaldi[22a], B. Ristić[51], E. Ritsch[32], I. Riu[13], F. Rizatdinova[115], E. Rizvi[78], C. Rizzi[13], S.H. Robertson[89,l], A. Robichaud-Veronneau[89], D. Robinson[30], J.E.M. Robinson[44], A. Robson[55], C. Roda[125a,125b], Y. Rodina[87], A. Rodriguez Perez[13], D. Rodriguez Rodriguez[167], S. Roe[32], C.S. Rogan[59], O. Røhne[120], A. Romaniouk[99], M. Romano[22a,22b], S.M. Romano Saez[36], E. Romero Adam[167], N. Rompotis[139], M. Ronzani[50], L. Roos[82], E. Ros[167], S. Rosati[133a], K. Rosbach[50], P. Rose[138], O. Rosenthal[142], V. Rossetti[147a,147b], E. Rossi[105a,105b], L.P. Rossi[52a], J.H.N. Rosten[30], R. Rosten[139], M. Rotaru[28b], I. Roth[172], J. Rothberg[139], D. Rousseau[118], C.R. Royon[137], A. Rozanov[87], Y. Rozen[153], X. Ruan[146c], F. Rubbo[144], I. Rubinskiy[44], V.I. Rud[100], M.S. Rudolph[159], F. Rühr[50], A. Ruiz-Martinez[32], Z. Rurikova[50], N.A. Rusakovich[67], A. Ruschke[101], H.L. Russell[139], J.P. Rutherfoord[7], N. Ruthmann[32], Y.F. Ryabov[124], M. Rybar[166], G. Rybkin[118], S. Ryu[6], A. Ryzhov[131], A.F. Saavedra[151], G. Sabato[108], S. Sacerdoti[29], H.F-W. Sadrozinski[138], R. Sadykov[67], F. Safai Tehrani[133a], P. Saha[109], M. Sahinsoy[60a], M. Saimpert[137], T. Saito[156], H. Sakamoto[156], Y. Sakurai[171], G. Salamanna[135a,135b], A. Salamon[134a,134b], J.E. Salazar Loyola[34b], D. Salek[108], P.H. Sales De Bruin[139], D. Salihagic[102], A. Salnikov[144], J. Salt[167], D. Salvatore[39a,39b], F. Salvatore[150], A. Salvucci[62a], A. Salzburger[32], D. Sammel[50], D. Sampsonidis[155], A. Sanchez[105a,105b], J. Sánchez[167], V. Sanchez Martinez[167], H. Sandaker[120], R.L. Sandbach[78], H.G. Sander[85], M.P. Sanders[101], M. Sandhoff[175], C. Sandoval[21], R. Sandstroem[102], D.P.C. Sankey[132], M. Sannino[52a,52b], A. Sansoni[49], C. Santoni[36], R. Santonico[134a,134b], H. Santos[127a], I. Santoyo Castillo[150], K. Sapp[126], A. Sapronov[67], J.G. Saraiva[127a,127d], B. Sarrazin[23], O. Sasaki[68], Y. Sasaki[156], K. Sato[161], G. Sauvage[5,*], E. Sauvan[5], G. Savage[79], P. Savard[159,d], C. Sawyer[132], L. Sawyer[81,p], J. Saxon[33], C. Sbarra[22a], A. Sbrizzi[22a,22b], T. Scanlon[80], D.A. Scannicchio[163], M. Scarcella[151], V. Scarfone[39a,39b], J. Schaarschmidt[172], P. Schacht[102], D. Schaefer[32], R. Schaefer[44], J. Schaeffer[85], S. Schaepe[23], S. Schaetzel[60b], U. Schäfer[85], A.C. Schaffer[118], D. Schaile[101], R.D. Schamberger[149], V. Scharf[60a], V.A. Schegelsky[124], D. Scheirich[130], M. Schernau[163], C. Schiavi[52a,52b], C. Schillo[50], M. Schioppa[39a,39b], S. Schlenker[32], K. Schmieden[32], C. Schmitt[85], S. Schmitt[44], S. Schmitz[85], B. Schneider[160a], Y.J. Schnellbach[76], U. Schnoor[50], L. Schoeffel[137], A. Schoening[60b], B.D. Schoenrock[92], E. Schopf[23], A.L.S. Schorlemmer[45], M. Schott[85], J. Schovancova[8], S. Schramm[51], M. Schreyer[174], N. Schuh[85], M.J. Schultens[23], H.-C. Schultz-Coulon[60a], H. Schulz[17], M. Schumacher[50], B.A. Schumm[138], Ph. Schune[137], C. Schwanenberger[86], A. Schwartzman[144], T.A. Schwarz[91], Ph. Schwegler[102], H. Schweiger[86], Ph. Schwemling[137], R. Schwienhorst[92], J. Schwindling[137], T. Schwindt[23], G. Sciolla[25], F. Scuri[125a,125b], F. Scutti[90], J. Searcy[91], P. Seema[23], S.C. Seidel[106], A. Seiden[138], F. Seifert[129], J.M. Seixas[26a], G. Sekhniaidze[105a], K. Sekhon[91], S.J. Sekula[42], D.M. Seliverstov[124,*], N. Semprini-Cesari[22a,22b], C. Serfon[120], L. Serin[118], L. Serkin[164a,164b], M. Sessa[135a,135b], R. Seuster[160a], H. Severini[114], T. Sfiligoj[77], F. Sforza[32], A. Sfyrla[51], E. Shabalina[56], N.W. Shaikh[147a,147b], L.Y. Shan[35a], R. Shang[166], J.T. Shank[24], M. Shapiro[16], P.B. Shatalov[98], K. Shaw[164a,164b], S.M. Shaw[86], A. Shcherbakova[147a,147b], C.Y. Shehu[150], P. Sherwood[80], L. Shi[152,ai], S. Shimizu[69], C.O. Shimmin[163], M. Shimojima[103], M. Shiyakova[67,aj], A. Shmeleva[97], D. Shoaleh Saadi[96], M.J. Shochet[33], S. Shojaii[93a,93b], S. Shrestha[112], E. Shulga[99], M.A. Shupe[7],

P. Sicho[128], P.E. Sidebo[148], O. Sidiropoulou[174], D. Sidorov[115], A. Sidoti[22a,22b], F. Siegert[46], Dj. Sijacki[14], J. Silva[127a,127d], S.B. Silverstein[147a], V. Simak[129], O. Simard[5], Lj. Simic[14], S. Simion[118], E. Simioni[85], B. Simmons[80], D. Simon[36], M. Simon[85], P. Sinervo[159], N.B. Sinev[117], M. Sioli[22a,22b], G. Siragusa[174], S.Yu. Sivoklokov[100], J. Sjölin[147a,147b], T.B. Sjursen[15], M.B. Skinner[74], H.P. Skottowe[59], P. Skubic[114], M. Slater[19], T. Slavicek[129], M. Slawinska[108], K. Sliwa[162], R. Slovak[130], V. Smakhtin[172], B.H. Smart[5], L. Smestad[15], S.Yu. Smirnov[99], Y. Smirnov[99], L.N. Smirnova[100,ak], O. Smirnova[83], M.N.K. Smith[37], R.W. Smith[37], M. Smizanska[74], K. Smolek[129], A.A. Snesarev[97], G. Snidero[78], S. Snyder[27], R. Sobie[169,l], F. Socher[46], A. Soffer[154], D.A. Soh[152,ai], G. Sokhrannyi[77], C.A. Solans Sanchez[32], M. Solar[129], E.Yu. Soldatov[99], U. Soldevila[167], A.A. Solodkov[131], A. Soloshenko[67], O.V. Solovyanov[131], V. Solovyev[124], P. Sommer[50], H. Son[162], H.Y. Song[35b,al], A. Sood[16], A. Sopczak[129], V. Sopko[129], V. Sorin[13], D. Sosa[60b], C.L. Sotiropoulou[125a,125b], R. Soualah[164a,164c], A.M. Soukharev[110,c], D. South[44], B.C. Sowden[79], S. Spagnolo[75a,75b], M. Spalla[125a,125b], M. Spangenberg[170], F. Spanò[79], D. Sperlich[17], F. Spettel[102], R. Spighi[22a], G. Spigo[32], L.A. Spiller[90], M. Spousta[130], R.D. St. Denis[55,*], A. Stabile[93a], J. Stahlman[123], R. Stamen[60a], S. Stamm[17], E. Stanecka[41], R.W. Stanek[6], C. Stanescu[135a], M. Stanescu-Bellu[44], M.M. Stanitzki[44], S. Stapnes[120], E.A. Starchenko[131], G.H. Stark[33], J. Stark[57], P. Staroba[128], P. Starovoitov[60a], S. Stärz[32], R. Staszewski[41], P. Steinberg[27], B. Stelzer[143], H.J. Stelzer[32], O. Stelzer-Chilton[160a], H. Stenzel[54], G.A. Stewart[55], J.A. Stillings[23], M.C. Stockton[89], M. Stoebe[89], G. Stoicea[28b], P. Stolte[56], S. Stonjek[102], A.R. Stradling[8], A. Straessner[46], M.E. Stramaglia[18], J. Strandberg[148], S. Strandberg[147a,147b], A. Strandlie[120], M. Strauss[114], P. Strizenec[145b], R. Ströhmer[174], D.M. Strom[117], R. Stroynowski[42], A. Strubig[107], S.A. Stucci[18], B. Stugu[15], N.A. Styles[44], D. Su[144], J. Su[126], R. Subramaniam[81], S. Suchek[60a], Y. Sugaya[119], M. Suk[129], V.V. Sulin[97], S. Sultansoy[4c], T. Sumida[70], S. Sun[59], X. Sun[35a], J.E. Sundermann[50], K. Suruliz[150], G. Susinno[39a,39b], M.R. Sutton[150], S. Suzuki[68], M. Svatos[128], M. Swiatlowski[33], I. Sykora[145a], T. Sykora[130], D. Ta[50], C. Taccini[135a,135b], K. Tackmann[44], J. Taenzer[159], A. Taffard[163], R. Tafirout[160a], N. Taiblum[154], H. Takai[27], R. Takashima[71], H. Takeda[69], T. Takeshita[141], Y. Takubo[68], M. Talby[87], A.A. Talyshev[110,c], J.Y.C. Tam[174], K.G. Tan[90], J. Tanaka[156], R. Tanaka[118], S. Tanaka[68], B.B. Tannenwald[112], S. Tapia Araya[34b], S. Tapprogge[85], S. Tarem[153], G.F. Tartarelli[93a], P. Tas[130], M. Tasevsky[128], T. Tashiro[70], E. Tassi[39a,39b], A. Tavares Delgado[127a,127b], Y. Tayalati[136d], A.C. Taylor[106], G.N. Taylor[90], P.T.E. Taylor[90], W. Taylor[160b], F.A. Teischinger[32], P. Teixeira-Dias[79], K.K. Temming[50], D. Temple[143], H. Ten Kate[32], P.K. Teng[152], J.J. Teoh[119], F. Tepel[175], S. Terada[68], K. Terashi[156], J. Terron[84], S. Terzo[102], M. Testa[49], R.J. Teuscher[159,l], T. Theveneaux-Pelzer[87], J.P. Thomas[19], J. Thomas-Wilsker[79], E.N. Thompson[37], P.D. Thompson[19], R.J. Thompson[86], A.S. Thompson[55], L.A. Thomsen[176], E. Thomson[123], M. Thomson[30], M.J. Tibbetts[16], R.E. Ticse Torres[87], V.O. Tikhomirov[97,am], Yu.A. Tikhonov[110,c], S. Timoshenko[99], P. Tipton[176], S. Tisserant[87], K. Todome[158], T. Todorov[5,*], S. Todorova-Nova[130], J. Tojo[72], S. Tokár[145a], K. Tokushuku[68], E. Tolley[59], L. Tomlinson[86], M. Tomoto[104], L. Tompkins[144,an], K. Toms[106], B. Tong[59], E. Torrence[117], H. Torres[143], E. Torró Pastor[139], J. Toth[87,ao], F. Touchard[87], D.R. Tovey[140], T. Trefzger[174], A. Tricoli[32], I.M. Trigger[160a], S. Trincaz-Duvoid[82], M.F. Tripiana[13], W. Trischuk[159], B. Trocmé[57], A. Trofymov[44], C. Troncon[93a], M. Trottier-McDonald[16], M. Trovatelli[169], L. Truong[164a,164b], M. Trzebinski[41], A. Trzupek[41], J.C-L. Tseng[121], P.V. Tsiareshka[94], G. Tsipolitis[10], N. Tsirintanis[9], S. Tsiskaridze[13], V. Tsiskaridze[50], E.G. Tskhadadze[53a], K.M. Tsui[62a], I.I. Tsukerman[98], V. Tsulaia[16], S. Tsuno[68], D. Tsybychev[149], A. Tudorache[28b], V. Tudorache[28b], A.N. Tuna[59], S.A. Tupputi[22a,22b], S. Turchikhin[100,ak], D. Turecek[129], D. Turgeman[172], R. Turra[93a,93b], A.J. Turvey[42], P.M. Tuts[37], M. Tyndel[132], G. Ucchielli[22a,22b], I. Ueda[156], R. Ueno[31], M. Ughetto[147a,147b], F. Ukegawa[161], G. Unal[32], A. Undrus[27], G. Unel[163], F.C. Ungaro[90], Y. Unno[68], C. Unverdorben[101], J. Urban[145b], P. Urquijo[90], P. Urrejola[85], G. Usai[8], A. Usanova[64], L. Vacavant[87], V. Vacek[129], B. Vachon[89], C. Valderanis[101], E. Valdes Santurio[147a,147b], N. Valencic[108], S. Valentinetti[22a,22b], A. Valero[167], L. Valery[13], S. Valkar[130], S. Vallecorsa[51], J.A. Valls Ferrer[167], W. Van Den Wollenberg[108],

P.C. Van Der Deijl[108], R. van der Geer[108], H. van der Graaf[108], N. van Eldik[153], P. van Gemmeren[6], J. Van Nieuwkoop[143], I. van Vulpen[108], M.C. van Woerden[32], M. Vanadia[133a,133b], W. Vandelli[32], R. Vanguri[123], A. Vaniachine[6], P. Vankov[108], G. Vardanyan[177], R. Vari[133a], E.W. Varnes[7], T. Varol[42], D. Varouchas[82], A. Vartapetian[8], K.E. Varvell[151], J.G. Vasquez[176], F. Vazeille[36], T. Vazquez Schroeder[89], J. Veatch[56], L.M. Veloce[159], F. Veloso[127a,127c], S. Veneziano[133a], A. Ventura[75a,75b], M. Venturi[169], N. Venturi[159], A. Venturini[25], V. Vercesi[122a], M. Verducci[133a,133b], W. Verkerke[108], J.C. Vermeulen[108], A. Vest[46,ap], M.C. Vetterli[143,d], O. Viazlo[83], I. Vichou[166], T. Vickey[140], O.E. Vickey Boeriu[140], G.H.A. Viehhauser[121], S. Viel[16], L. Vigani[121], R. Vigne[64], M. Villa[22a,22b], M. Villaplana Perez[93a,93b], E. Vilucchi[49], M.G. Vincter[31], V.B. Vinogradov[67], C. Vittori[22a,22b], I. Vivarelli[150], S. Vlachos[10], M. Vlasak[129], M. Vogel[175], P. Vokac[129], G. Volpi[125a,125b], M. Volpi[90], H. von der Schmitt[102], E. von Toerne[23], V. Vorobel[130], K. Vorobev[99], M. Vos[167], R. Voss[32], J.H. Vossebeld[76], N. Vranjes[14], M. Vranjes Milosavljevic[14], V. Vrba[128], M. Vreeswijk[108], R. Vuillermet[32], I. Vukotic[33], Z. Vykydal[129], P. Wagner[23], W. Wagner[175], H. Wahlberg[73], S. Wahrmund[46], J. Wakabayashi[104], J. Walder[74], R. Walker[101], W. Walkowiak[142], V. Wallangen[147a,147b], C. Wang[152], C. Wang[35d,87], F. Wang[173], H. Wang[16], H. Wang[42], J. Wang[44], J. Wang[151], K. Wang[89], R. Wang[6], S.M. Wang[152], T. Wang[23], T. Wang[37], X. Wang[176], C. Wanotayaroj[117], A. Warburton[89], C.P. Ward[30], D.R. Wardrope[80], A. Washbrook[48], P.M. Watkins[19], A.T. Watson[19], I.J. Watson[151], M.F. Watson[19], G. Watts[139], S. Watts[86], B.M. Waugh[80], S. Webb[85], M.S. Weber[18], S.W. Weber[174], J.S. Webster[6], A.R. Weidberg[121], B. Weinert[63], J. Weingarten[56], C. Weiser[50], H. Weits[108], P.S. Wells[32], T. Wenaus[27], T. Wengler[32], S. Wenig[32], N. Wermes[23], M. Werner[50], P. Werner[32], M. Wessels[60a], J. Wetter[162], K. Whalen[117], N.L. Whallon[139], A.M. Wharton[74], A. White[8], M.J. White[1], R. White[34b], S. White[125a,125b], D. Whiteson[163], F.J. Wickens[132], W. Wiedenmann[173], M. Wielers[132], P. Wienemann[23], C. Wiglesworth[38], L.A.M. Wiik-Fuchs[23], A. Wildauer[102], F. Wilk[86], H.G. Wilkens[32], H.H. Williams[123], S. Williams[108], C. Willis[92], S. Willocq[88], J.A. Wilson[19], I. Wingerter-Seez[5], F. Winklmeier[117], O.J. Winston[150], B.T. Winter[23], M. Wittgen[144], J. Wittkowski[101], S.J. Wollstadt[85], M.W. Wolter[41], H. Wolters[127a,127c], B.K. Wosiek[41], J. Wotschack[32], M.J. Woudstra[86], K.W. Wozniak[41], M. Wu[57], M. Wu[33], S.L. Wu[173], X. Wu[51], Y. Wu[91], T.R. Wyatt[86], B.M. Wynne[48], S. Xella[38], D. Xu[35a], L. Xu[27], B. Yabsley[151], S. Yacoob[146a], R. Yakabe[69], D. Yamaguchi[158], Y. Yamaguchi[119], A. Yamamoto[68], S. Yamamoto[156], T. Yamanaka[156], K. Yamauchi[104], Y. Yamazaki[69], Z. Yan[24], H. Yang[35e], H. Yang[173], Y. Yang[152], Z. Yang[15], W-M. Yao[16], Y.C. Yap[82], Y. Yasu[68], E. Yatsenko[5], K.H. Yau Wong[23], J. Ye[42], S. Ye[27], I. Yeletskikh[67], A.L. Yen[59], E. Yildirim[44], K. Yorita[171], R. Yoshida[6], K. Yoshihara[123], C. Young[144], C.J.S. Young[32], S. Youssef[24], D.R. Yu[16], J. Yu[8], J.M. Yu[91], J. Yu[66], L. Yuan[69], S.P.Y. Yuen[23], I. Yusuff[30,aq], B. Zabinski[41], R. Zaidan[35d], A.M. Zaitsev[131,ad], N. Zakharchuk[44], J. Zalieckas[15], A. Zaman[149], S. Zambito[59], L. Zanello[133a,133b], D. Zanzi[90], C. Zeitnitz[175], M. Zeman[129], A. Zemla[40a], J.C. Zeng[166], Q. Zeng[144], K. Zengel[25], O. Zenin[131], T. Ženiš[145a], D. Zerwas[118], D. Zhang[91], F. Zhang[173], G. Zhang[35b,al], H. Zhang[35c], J. Zhang[6], L. Zhang[50], R. Zhang[23], R. Zhang[35b,ar], X. Zhang[35d], Z. Zhang[118], X. Zhao[42], Y. Zhao[35d], Z. Zhao[35b], A. Zhemchugov[67], J. Zhong[121], B. Zhou[91], C. Zhou[47], L. Zhou[37], L. Zhou[42], M. Zhou[149], N. Zhou[35f], C.G. Zhu[35d], H. Zhu[35a], J. Zhu[91], Y. Zhu[35b], X. Zhuang[35a], K. Zhukov[97], A. Zibell[174], D. Zieminska[63], N.I. Zimine[67], C. Zimmermann[85], S. Zimmermann[50], Z. Zinonos[56], M. Zinser[85], M. Ziolkowski[142], L. Živković[14], G. Zobernig[173], A. Zoccoli[22a,22b], M. zur Nedden[17], G. Zurzolo[105a,105b], L. Zwalinski[32].

[1] Department of Physics, University of Adelaide, Adelaide, Australia

[2] Physics Department, SUNY Albany, Albany NY, United States of America

[3] Department of Physics, University of Alberta, Edmonton AB, Canada

[4] [(a)] Department of Physics, Ankara University, Ankara; [(b)] Istanbul Aydin University, Istanbul; [(c)] Division of Physics, TOBB University of Economics and Technology, Ankara, Turkey

[5] LAPP, CNRS/IN2P3 and Université Savoie Mont Blanc, Annecy-le-Vieux, France
[6] High Energy Physics Division, Argonne National Laboratory, Argonne IL, United States of America
[7] Department of Physics, University of Arizona, Tucson AZ, United States of America
[8] Department of Physics, The University of Texas at Arlington, Arlington TX, United States of America
[9] Physics Department, University of Athens, Athens, Greece
[10] Physics Department, National Technical University of Athens, Zografou, Greece
[11] Department of Physics, The University of Texas at Austin, Austin TX, United States of America
[12] Institute of Physics, Azerbaijan Academy of Sciences, Baku, Azerbaijan
[13] Institut de Física d'Altes Energies (IFAE), The Barcelona Institute of Science and Technology, Barcelona, Spain, Spain
[14] Institute of Physics, University of Belgrade, Belgrade, Serbia
[15] Department for Physics and Technology, University of Bergen, Bergen, Norway
[16] Physics Division, Lawrence Berkeley National Laboratory and University of California, Berkeley CA, United States of America
[17] Department of Physics, Humboldt University, Berlin, Germany
[18] Albert Einstein Center for Fundamental Physics and Laboratory for High Energy Physics, University of Bern, Bern, Switzerland
[19] School of Physics and Astronomy, University of Birmingham, Birmingham, United Kingdom
[20] [(a)] Department of Physics, Bogazici University, Istanbul; [(b)] Department of Physics Engineering, Gaziantep University, Gaziantep; [(d)] Istanbul Bilgi University, Faculty of Engineering and Natural Sciences, Istanbul,Turkey; [(e)] Bahcesehir University, Faculty of Engineering and Natural Sciences, Istanbul, Turkey, Turkey
[21] Centro de Investigaciones, Universidad Antonio Narino, Bogota, Colombia
[22] [(a)] INFN Sezione di Bologna; [(b)] Dipartimento di Fisica e Astronomia, Università di Bologna, Bologna, Italy
[23] Physikalisches Institut, University of Bonn, Bonn, Germany
[24] Department of Physics, Boston University, Boston MA, United States of America
[25] Department of Physics, Brandeis University, Waltham MA, United States of America
[26] [(a)] Universidade Federal do Rio De Janeiro COPPE/EE/IF, Rio de Janeiro; [(b)] Electrical Circuits Department, Federal University of Juiz de Fora (UFJF), Juiz de Fora; [(c)] Federal University of Sao Joao del Rei (UFSJ), Sao Joao del Rei; [(d)] Instituto de Fisica, Universidade de Sao Paulo, Sao Paulo, Brazil
[27] Physics Department, Brookhaven National Laboratory, Upton NY, United States of America
[28] [(a)] Transilvania University of Brasov, Brasov, Romania; [(b)] National Institute of Physics and Nuclear Engineering, Bucharest; [(c)] National Institute for Research and Development of Isotopic and Molecular Technologies, Physics Department, Cluj Napoca; [(d)] University Politehnica Bucharest, Bucharest; [(e)] West University in Timisoara, Timisoara, Romania
[29] Departamento de Física, Universidad de Buenos Aires, Buenos Aires, Argentina
[30] Cavendish Laboratory, University of Cambridge, Cambridge, United Kingdom
[31] Department of Physics, Carleton University, Ottawa ON, Canada
[32] CERN, Geneva, Switzerland
[33] Enrico Fermi Institute, University of Chicago, Chicago IL, United States of America
[34] [(a)] Departamento de Física, Pontificia Universidad Católica de Chile, Santiago; [(b)] Departamento de Física, Universidad Técnica Federico Santa María, Valparaíso, Chile
[35] [(a)] Institute of High Energy Physics, Chinese Academy of Sciences, Beijing; [(b)] Department of Modern Physics, University of Science and Technology of China, Anhui; [(c)] Department of Physics, Nanjing University, Jiangsu; [(d)] School of Physics, Shandong University, Shandong; [(e)] Department of Physics and Astronomy, Shanghai Key Laboratory for Particle Physics and Cosmology, Shanghai Jiao

Tong University, Shanghai; (also affiliated with PKU-CHEP); [f] Physics Department, Tsinghua University, Beijing 100084, China
[36] Laboratoire de Physique Corpusculaire, Clermont Université and Université Blaise Pascal and CNRS/IN2P3, Clermont-Ferrand, France
[37] Nevis Laboratory, Columbia University, Irvington NY, United States of America
[38] Niels Bohr Institute, University of Copenhagen, Kobenhavn, Denmark
[39] [a] INFN Gruppo Collegato di Cosenza, Laboratori Nazionali di Frascati; [b] Dipartimento di Fisica, Università della Calabria, Rende, Italy
[40] [a] AGH University of Science and Technology, Faculty of Physics and Applied Computer Science, Krakow; [b] Marian Smoluchowski Institute of Physics, Jagiellonian University, Krakow, Poland
[41] Institute of Nuclear Physics Polish Academy of Sciences, Krakow, Poland
[42] Physics Department, Southern Methodist University, Dallas TX, United States of America
[43] Physics Department, University of Texas at Dallas, Richardson TX, United States of America
[44] DESY, Hamburg and Zeuthen, Germany
[45] Institut für Experimentelle Physik IV, Technische Universität Dortmund, Dortmund, Germany
[46] Institut für Kern- und Teilchenphysik, Technische Universität Dresden, Dresden, Germany
[47] Department of Physics, Duke University, Durham NC, United States of America
[48] SUPA - School of Physics and Astronomy, University of Edinburgh, Edinburgh, United Kingdom
[49] INFN Laboratori Nazionali di Frascati, Frascati, Italy
[50] Fakultät für Mathematik und Physik, Albert-Ludwigs-Universität, Freiburg, Germany
[51] Section de Physique, Université de Genève, Geneva, Switzerland
[52] [a] INFN Sezione di Genova; [b] Dipartimento di Fisica, Università di Genova, Genova, Italy
[53] [a] E. Andronikashvili Institute of Physics, Iv. Javakhishvili Tbilisi State University, Tbilisi; [b] High Energy Physics Institute, Tbilisi State University, Tbilisi, Georgia
[54] II Physikalisches Institut, Justus-Liebig-Universität Giessen, Giessen, Germany
[55] SUPA - School of Physics and Astronomy, University of Glasgow, Glasgow, United Kingdom
[56] II Physikalisches Institut, Georg-August-Universität, Göttingen, Germany
[57] Laboratoire de Physique Subatomique et de Cosmologie, Université Grenoble-Alpes, CNRS/IN2P3, Grenoble, France
[58] Department of Physics, Hampton University, Hampton VA, United States of America
[59] Laboratory for Particle Physics and Cosmology, Harvard University, Cambridge MA, United States of America
[60] [a] Kirchhoff-Institut für Physik, Ruprecht-Karls-Universität Heidelberg, Heidelberg; [b] Physikalisches Institut, Ruprecht-Karls-Universität Heidelberg, Heidelberg; [c] ZITI Institut für technische Informatik, Ruprecht-Karls-Universität Heidelberg, Mannheim, Germany
[61] Faculty of Applied Information Science, Hiroshima Institute of Technology, Hiroshima, Japan
[62] [a] Department of Physics, The Chinese University of Hong Kong, Shatin, N.T., Hong Kong; [b] Department of Physics, The University of Hong Kong, Hong Kong; [c] Department of Physics, The Hong Kong University of Science and Technology, Clear Water Bay, Kowloon, Hong Kong, China
[63] Department of Physics, Indiana University, Bloomington IN, United States of America
[64] Institut für Astro- und Teilchenphysik, Leopold-Franzens-Universität, Innsbruck, Austria
[65] University of Iowa, Iowa City IA, United States of America
[66] Department of Physics and Astronomy, Iowa State University, Ames IA, United States of America
[67] Joint Institute for Nuclear Research, JINR Dubna, Dubna, Russia
[68] KEK, High Energy Accelerator Research Organization, Tsukuba, Japan
[69] Graduate School of Science, Kobe University, Kobe, Japan
[70] Faculty of Science, Kyoto University, Kyoto, Japan

[71] Kyoto University of Education, Kyoto, Japan
[72] Department of Physics, Kyushu University, Fukuoka, Japan
[73] Instituto de Física La Plata, Universidad Nacional de La Plata and CONICET, La Plata, Argentina
[74] Physics Department, Lancaster University, Lancaster, United Kingdom
[75] [(a)] INFN Sezione di Lecce; [(b)] Dipartimento di Matematica e Fisica, Università del Salento, Lecce, Italy
[76] Oliver Lodge Laboratory, University of Liverpool, Liverpool, United Kingdom
[77] Department of Physics, Jožef Stefan Institute and University of Ljubljana, Ljubljana, Slovenia
[78] School of Physics and Astronomy, Queen Mary University of London, London, United Kingdom
[79] Department of Physics, Royal Holloway University of London, Surrey, United Kingdom
[80] Department of Physics and Astronomy, University College London, London, United Kingdom
[81] Louisiana Tech University, Ruston LA, United States of America
[82] Laboratoire de Physique Nucléaire et de Hautes Energies, UPMC and Université Paris-Diderot and CNRS/IN2P3, Paris, France
[83] Fysiska institutionen, Lunds universitet, Lund, Sweden
[84] Departamento de Fisica Teorica C-15, Universidad Autonoma de Madrid, Madrid, Spain
[85] Institut für Physik, Universität Mainz, Mainz, Germany
[86] School of Physics and Astronomy, University of Manchester, Manchester, United Kingdom
[87] CPPM, Aix-Marseille Université and CNRS/IN2P3, Marseille, France
[88] Department of Physics, University of Massachusetts, Amherst MA, United States of America
[89] Department of Physics, McGill University, Montreal QC, Canada
[90] School of Physics, University of Melbourne, Victoria, Australia
[91] Department of Physics, The University of Michigan, Ann Arbor MI, United States of America
[92] Department of Physics and Astronomy, Michigan State University, East Lansing MI, United States of America
[93] [(a)] INFN Sezione di Milano; [(b)] Dipartimento di Fisica, Università di Milano, Milano, Italy
[94] B.I. Stepanov Institute of Physics, National Academy of Sciences of Belarus, Minsk, Republic of Belarus
[95] National Scientific and Educational Centre for Particle and High Energy Physics, Minsk, Republic of Belarus
[96] Group of Particle Physics, University of Montreal, Montreal QC, Canada
[97] P.N. Lebedev Physical Institute of the Russian Academy of Sciences, Moscow, Russia
[98] Institute for Theoretical and Experimental Physics (ITEP), Moscow, Russia
[99] National Research Nuclear University MEPhI, Moscow, Russia
[100] D.V. Skobeltsyn Institute of Nuclear Physics, M.V. Lomonosov Moscow State University, Moscow, Russia
[101] Fakultät für Physik, Ludwig-Maximilians-Universität München, München, Germany
[102] Max-Planck-Institut für Physik (Werner-Heisenberg-Institut), München, Germany
[103] Nagasaki Institute of Applied Science, Nagasaki, Japan
[104] Graduate School of Science and Kobayashi-Maskawa Institute, Nagoya University, Nagoya, Japan
[105] [(a)] INFN Sezione di Napoli; [(b)] Dipartimento di Fisica, Università di Napoli, Napoli, Italy
[106] Department of Physics and Astronomy, University of New Mexico, Albuquerque NM, United States of America
[107] Institute for Mathematics, Astrophysics and Particle Physics, Radboud University Nijmegen/Nikhef, Nijmegen, Netherlands
[108] Nikhef National Institute for Subatomic Physics and University of Amsterdam, Amsterdam, Netherlands

[109] Department of Physics, Northern Illinois University, DeKalb IL, United States of America
[110] Budker Institute of Nuclear Physics, SB RAS, Novosibirsk, Russia
[111] Department of Physics, New York University, New York NY, United States of America
[112] Ohio State University, Columbus OH, United States of America
[113] Faculty of Science, Okayama University, Okayama, Japan
[114] Homer L. Dodge Department of Physics and Astronomy, University of Oklahoma, Norman OK, United States of America
[115] Department of Physics, Oklahoma State University, Stillwater OK, United States of America
[116] Palacký University, RCPTM, Olomouc, Czech Republic
[117] Center for High Energy Physics, University of Oregon, Eugene OR, United States of America
[118] LAL, Univ. Paris-Sud, CNRS/IN2P3, Université Paris-Saclay, Orsay, France
[119] Graduate School of Science, Osaka University, Osaka, Japan
[120] Department of Physics, University of Oslo, Oslo, Norway
[121] Department of Physics, Oxford University, Oxford, United Kingdom
[122] [(a)] INFN Sezione di Pavia; [(b)] Dipartimento di Fisica, Università di Pavia, Pavia, Italy
[123] Department of Physics, University of Pennsylvania, Philadelphia PA, United States of America
[124] National Research Centre "Kurchatov Institute" B.P.Konstantinov Petersburg Nuclear Physics Institute, St. Petersburg, Russia
[125] [(a)] INFN Sezione di Pisa; [(b)] Dipartimento di Fisica E. Fermi, Università di Pisa, Pisa, Italy
[126] Department of Physics and Astronomy, University of Pittsburgh, Pittsburgh PA, United States of America
[127] [(a)] Laboratório de Instrumentação e Física Experimental de Partículas - LIP, Lisboa; [(b)] Faculdade de Ciências, Universidade de Lisboa, Lisboa; [(c)] Department of Physics, University of Coimbra, Coimbra; [(d)] Centro de Física Nuclear da Universidade de Lisboa, Lisboa; [(e)] Departamento de Fisica, Universidade do Minho, Braga; [(f)] Departamento de Fisica Teorica y del Cosmos and CAFPE, Universidad de Granada, Granada (Spain); [(g)] Dep Fisica and CEFITEC of Faculdade de Ciencias e Tecnologia, Universidade Nova de Lisboa, Caparica, Portugal
[128] Institute of Physics, Academy of Sciences of the Czech Republic, Praha, Czech Republic
[129] Czech Technical University in Prague, Praha, Czech Republic
[130] Faculty of Mathematics and Physics, Charles University in Prague, Praha, Czech Republic
[131] State Research Center Institute for High Energy Physics (Protvino), NRC KI, Russia
[132] Particle Physics Department, Rutherford Appleton Laboratory, Didcot, United Kingdom
[133] [(a)] INFN Sezione di Roma; [(b)] Dipartimento di Fisica, Sapienza Università di Roma, Roma, Italy
[134] [(a)] INFN Sezione di Roma Tor Vergata; [(b)] Dipartimento di Fisica, Università di Roma Tor Vergata, Roma, Italy
[135] [(a)] INFN Sezione di Roma Tre; [(b)] Dipartimento di Matematica e Fisica, Università Roma Tre, Roma, Italy
[136] [(a)] Faculté des Sciences Ain Chock, Réseau Universitaire de Physique des Hautes Energies - Université Hassan II, Casablanca; [(b)] Centre National de l'Energie des Sciences Techniques Nucleaires, Rabat; [(c)] Faculté des Sciences Semlalia, Université Cadi Ayyad, LPHEA-Marrakech; [(d)] Faculté des Sciences, Université Mohamed Premier and LPTPM, Oujda; [(e)] Faculté des sciences, Université Mohammed V, Rabat, Morocco
[137] DSM/IRFU (Institut de Recherches sur les Lois Fondamentales de l'Univers), CEA Saclay (Commissariat à l'Energie Atomique et aux Energies Alternatives), Gif-sur-Yvette, France
[138] Santa Cruz Institute for Particle Physics, University of California Santa Cruz, Santa Cruz CA, United States of America
[139] Department of Physics, University of Washington, Seattle WA, United States of America

[140] Department of Physics and Astronomy, University of Sheffield, Sheffield, United Kingdom
[141] Department of Physics, Shinshu University, Nagano, Japan
[142] Fachbereich Physik, Universität Siegen, Siegen, Germany
[143] Department of Physics, Simon Fraser University, Burnaby BC, Canada
[144] SLAC National Accelerator Laboratory, Stanford CA, United States of America
[145] [(a)] Faculty of Mathematics, Physics & Informatics, Comenius University, Bratislava; [(b)] Department of Subnuclear Physics, Institute of Experimental Physics of the Slovak Academy of Sciences, Kosice, Slovak Republic
[146] [(a)] Department of Physics, University of Cape Town, Cape Town; [(b)] Department of Physics, University of Johannesburg, Johannesburg; [(c)] School of Physics, University of the Witwatersrand, Johannesburg, South Africa
[147] [(a)] Department of Physics, Stockholm University; [(b)] The Oskar Klein Centre, Stockholm, Sweden
[148] Physics Department, Royal Institute of Technology, Stockholm, Sweden
[149] Departments of Physics & Astronomy and Chemistry, Stony Brook University, Stony Brook NY, United States of America
[150] Department of Physics and Astronomy, University of Sussex, Brighton, United Kingdom
[151] School of Physics, University of Sydney, Sydney, Australia
[152] Institute of Physics, Academia Sinica, Taipei, Taiwan
[153] Department of Physics, Technion: Israel Institute of Technology, Haifa, Israel
[154] Raymond and Beverly Sackler School of Physics and Astronomy, Tel Aviv University, Tel Aviv, Israel
[155] Department of Physics, Aristotle University of Thessaloniki, Thessaloniki, Greece
[156] International Center for Elementary Particle Physics and Department of Physics, The University of Tokyo, Tokyo, Japan
[157] Graduate School of Science and Technology, Tokyo Metropolitan University, Tokyo, Japan
[158] Department of Physics, Tokyo Institute of Technology, Tokyo, Japan
[159] Department of Physics, University of Toronto, Toronto ON, Canada
[160] [(a)] TRIUMF, Vancouver BC; [(b)] Department of Physics and Astronomy, York University, Toronto ON, Canada
[161] Faculty of Pure and Applied Sciences, and Center for Integrated Research in Fundamental Science and Engineering, University of Tsukuba, Tsukuba, Japan
[162] Department of Physics and Astronomy, Tufts University, Medford MA, United States of America
[163] Department of Physics and Astronomy, University of California Irvine, Irvine CA, United States of America
[164] [(a)] INFN Gruppo Collegato di Udine, Sezione di Trieste, Udine; [(b)] ICTP, Trieste; [(c)] Dipartimento di Chimica, Fisica e Ambiente, Università di Udine, Udine, Italy
[165] Department of Physics and Astronomy, University of Uppsala, Uppsala, Sweden
[166] Department of Physics, University of Illinois, Urbana IL, United States of America
[167] Instituto de Fisica Corpuscular (IFIC) and Departamento de Fisica Atomica, Molecular y Nuclear and Departamento de Ingeniería Electrónica and Instituto de Microelectrónica de Barcelona (IMB-CNM), University of Valencia and CSIC, Valencia, Spain
[168] Department of Physics, University of British Columbia, Vancouver BC, Canada
[169] Department of Physics and Astronomy, University of Victoria, Victoria BC, Canada
[170] Department of Physics, University of Warwick, Coventry, United Kingdom
[171] Waseda University, Tokyo, Japan
[172] Department of Particle Physics, The Weizmann Institute of Science, Rehovot, Israel
[173] Department of Physics, University of Wisconsin, Madison WI, United States of America

[174] Fakultät für Physik und Astronomie, Julius-Maximilians-Universität, Würzburg, Germany
[175] Fakultät für Mathematik und Naturwissenschaften, Fachgruppe Physik, Bergische Universität Wuppertal, Wuppertal, Germany
[176] Department of Physics, Yale University, New Haven CT, United States of America
[177] Yerevan Physics Institute, Yerevan, Armenia
[178] Centre de Calcul de l'Institut National de Physique Nucléaire et de Physique des Particules (IN2P3), Villeurbanne, France
[a] Also at Department of Physics, King's College London, London, United Kingdom
[b] Also at Institute of Physics, Azerbaijan Academy of Sciences, Baku, Azerbaijan
[c] Also at Novosibirsk State University, Novosibirsk, Russia
[d] Also at TRIUMF, Vancouver BC, Canada
[e] Also at Department of Physics & Astronomy, University of Louisville, Louisville, KY, United States of America
[f] Also at Department of Physics, California State University, Fresno CA, United States of America
[g] Also at Department of Physics, University of Fribourg, Fribourg, Switzerland
[h] Also at Departament de Fisica de la Universitat Autonoma de Barcelona, Barcelona, Spain
[i] Also at Departamento de Fisica e Astronomia, Faculdade de Ciencias, Universidade do Porto, Portugal
[j] Also at Tomsk State University, Tomsk, Russia
[k] Also at Universita di Napoli Parthenope, Napoli, Italy
[l] Also at Institute of Particle Physics (IPP), Canada
[m] Also at Department of Physics, St. Petersburg State Polytechnical University, St. Petersburg, Russia
[n] Also at Department of Physics, The University of Michigan, Ann Arbor MI, United States of America
[o] Also at Centre for High Performance Computing, CSIR Campus, Rosebank, Cape Town, South Africa
[p] Also at Louisiana Tech University, Ruston LA, United States of America
[q] Also at Institucio Catalana de Recerca i Estudis Avancats, ICREA, Barcelona, Spain
[r] Also at Graduate School of Science, Osaka University, Osaka, Japan
[s] Also at Department of Physics, National Tsing Hua University, Taiwan
[t] Also at Institute for Mathematics, Astrophysics and Particle Physics, Radboud University Nijmegen/Nikhef, Nijmegen, Netherlands
[u] Also at Department of Physics, The University of Texas at Austin, Austin TX, United States of America
[v] Also at Institute of Theoretical Physics, Ilia State University, Tbilisi, Georgia
[w] Also at CERN, Geneva, Switzerland
[x] Also at Georgian Technical University (GTU),Tbilisi, Georgia
[y] Also at Ochadai Academic Production, Ochanomizu University, Tokyo, Japan
[z] Also at Manhattan College, New York NY, United States of America
[aa] Also at Hellenic Open University, Patras, Greece
[ab] Also at Academia Sinica Grid Computing, Institute of Physics, Academia Sinica, Taipei, Taiwan
[ac] Also at School of Physics, Shandong University, Shandong, China
[ad] Also at Moscow Institute of Physics and Technology State University, Dolgoprudny, Russia
[ae] Also at Section de Physique, Université de Genève, Geneva, Switzerland
[af] Also at Eotvos Lorand University, Budapest, Hungary
[ag] Also at International School for Advanced Studies (SISSA), Trieste, Italy
[ah] Also at Department of Physics and Astronomy, University of South Carolina, Columbia SC, United States of America
[ai] Also at School of Physics and Engineering, Sun Yat-sen University, Guangzhou, China
[aj] Also at Institute for Nuclear Research and Nuclear Energy (INRNE) of the Bulgarian Academy of

Sciences, Sofia, Bulgaria
[ak] Also at Faculty of Physics, M.V.Lomonosov Moscow State University, Moscow, Russia
[al] Also at Institute of Physics, Academia Sinica, Taipei, Taiwan
[am] Also at National Research Nuclear University MEPhI, Moscow, Russia
[an] Also at Department of Physics, Stanford University, Stanford CA, United States of America
[ao] Also at Institute for Particle and Nuclear Physics, Wigner Research Centre for Physics, Budapest, Hungary
[ap] Also at Flensburg University of Applied Sciences, Flensburg, Germany
[aq] Also at University of Malaya, Department of Physics, Kuala Lumpur, Malaysia
[ar] Also at CPPM, Aix-Marseille Université and CNRS/IN2P3, Marseille, France
[*] Deceased